

Deep Bayesian Quadrature Policy Optimization

Akella Ravi Tej¹, Kamyar Azizzadenesheli³, Mohammad Ghavamzadeh²,
Anima Anandkumar³, Yisong Yue³

¹ Indian Institute of Technology Roorkee, ² Google Research, ³ Caltech
ravitej.akella@gmail.com, ghavamza@google.com
{kazizzad, yyue, anima}@caltech.edu

Abstract

We study the problem of obtaining accurate policy gradient estimates. This challenge manifests in how best to estimate the policy gradient integral equation using a finite number of samples. Monte-Carlo methods have been the default choice for this purpose, despite suffering from high variance in the gradient estimates. On the other hand, more sample efficient alternatives like Bayesian quadrature methods are less scalable due to their high computational complexity. In this work, we propose deep Bayesian quadrature policy gradient (DBQPG), a computationally efficient high-dimensional generalization of Bayesian quadrature, to estimate the policy gradient integral equation. We show that DBQPG can substitute Monte-Carlo estimation in policy gradient methods, and demonstrate its effectiveness on a set of continuous control benchmarks for robotic locomotion. In comparison to Monte-Carlo estimation, DBQPG provides (i) more accurate gradient estimates with a significantly lower variance, (ii) a consistent improvement in the sample complexity and average return for several on-policy deep policy gradient algorithms, and, (iii) a methodological way to quantify the uncertainty in gradient estimation that can be incorporated to further improve the performance.

1 Introduction

Policy gradient (PG) is a reinforcement learning (RL) approach that directly optimizes the agent’s policies by operating on the gradient of their expected return (Sutton et al., 2000; Baxter & Bartlett, 2000). The use of deep neural networks for the policy class has recently demonstrated a series of success for PG methods (Lillicrap et al., 2015; Schulman et al., 2015) on high-dimensional continuous control benchmarks, such as MuJoCo (Todorov et al., 2012). However, the derivation and analysis of the aforementioned methods mainly rely on access to the expected return and its true gradient. In general, RL agents do not have access to the true gradient of the expected return, i.e., the gradient of integration over returns; instead, they have access to its empirical estimate from sampled trajectories. Monte-Carlo (MC) sampling (Metropolis & Ulam, 1949) is a widely used point estimation method for numerically approximating this integration (Williams, 1992). A variety of advanced methods have been proposed to improve the statistical efficiency of such empirical estimation. These methods mainly exploit the structure of Markov decision processes (MDP) (Puterman, 2014), estimate the value function, and subsequently utilize it in the estimation of the PG (Sutton et al., 2000; Schulman et al., 2016). However, the high variance in MC estimation imposes a high sample complexity requirement for PG algorithms (Rubinstein, 1969; Ilyas et al., 2018).

An alternate approach to approximate integrals in probabilistic numerics is Bayesian Quadrature (BQ) (O’Hagan, 1991). Under mild regularity assumptions, BQ methods offer impressive empirical advances and strictly faster convergence rates (Kanagawa et al., 2016). Typically, the integrand in BQ is modeled using a Gaussian process (GP), such that the linearity of the integral operator provides a Gaussian posterior over the integral. Thus, in addition to a point estimate of PG, these methods also quantify the uncertainty in gradient estimation, a missing piece in MC approaches.

In RL, the BQ machinery can be used to obtain a Gaussian approximation of the PG integral, by placing a GP prior over the action-value function. Ghavamzadeh & Engel (2007) showed that using a Fisher kernel in BQ provides closed-form expressions for the posterior moments of gradient integration. While the authors demonstrate a superior performance of BQ over MC using a small policy network on simple environments, the prohibitive computational complexity of BQ prevents scaling to large non-linear policies (> 1000 trainable parameters) and high-dimensional domains.

In this paper, we propose deep Bayesian quadrature policy gradient (DBQPG), a scalable BQ-based PG method for computing the gradient of the expected return. DBQPG uses GPs to model the action-value function, and without explicitly constructing the action-value function, returns a Gaussian approximation of the gradient, represented by a mean vector (gradient estimate) and covariance (uncertainty). The practical DBQPG algorithm utilizes the recent advances in structured kernel interpolations (Wilson & Nickisch, 2015) for computational efficiency and GPU acceleration for fast kernel learning (Gardner et al., 2018).

Recently, Ilyas et al. (2018) argued that the MC gradient estimation in PG methods is undesirably inaccurate. After studying the empirical variance in the estimated gradients and their cosine similarity with respect to the true gradients, they conclude that the MC method requires inordinate sample sizes to produce reasonably accurate PG estimates. Compared to MC sampling, we show that DBQPG estimates gradients that are both much closer to the true gradient, and with much lower variance. Therefore, DBQPG can favorably substitute MC estimation subroutine in a variety of PG methods. Specifically, we show that replacing the MC estimation subroutine with DBQPG provides a significant improvement in the sample complexity and average return for vanilla PG (Sutton et al., 2000), natural policy gradient (NPG) (Kakade, 2001) and trust region policy optimization (TRPO) (Schulman et al., 2015) algorithms, across 7 diverse MuJoCo environments.

Finally, we propose uncertainty aware PG (UAPG), a novel policy gradient method that utilizes the uncertainty in the gradient estimation for computing reliable policy updates. A majority of PG algorithms (Kakade, 2001; Schulman et al., 2015) are derived assuming access to true gradients and therefore do not take the uncertainty in gradient estimation, due to finite sample size, into account. However, one can obtain more reliable policy updates by lowering the stepsize along the directions of high estimation uncertainty and vice versa. UAPG captures this intuition by using uncertainty along the principal directions of PG’s covariance matrix to adjust the stepsize of the corresponding gradient components. Empirically, we show that UAPG further improves over DBQPG, which uses a uniform stepsize for all the gradient components regardless of their respective estimation uncertainties. Our implementation of DBQPG and UAPG methods is available online: <https://github.com/Akella17/Deep-Bayesian-Quadrature-Policy-Optimization>.

2 Preliminaries

Consider a Markov decision process $\langle \mathcal{S}, \mathcal{A}, P, r, \rho_0, \gamma \rangle$, where \mathcal{S} is the state-space, \mathcal{A} is the action-space, $P : \mathcal{S} \times \mathcal{A} \rightarrow \Delta_{\mathcal{S}}$ is the transition kernel that maps each state-action pair to a distribution

over the states $\Delta_{\mathcal{S}}$, $r : \mathcal{S} \times \mathcal{A} \rightarrow \mathbb{R}$ is the reward kernel, $\rho_0 : \mathcal{S} \rightarrow \Delta_{\mathcal{S}}$ is the initial state distribution, and $\gamma \in [0, 1)$ is the discount factor. We denote by $\pi_{\theta} : \mathcal{S} \rightarrow \Delta_{\mathcal{A}}$ a stochastic parameterized policy with parameters $\theta \in \Theta$. The MDP controlled by the policy π_{θ} induces a Markov chain over state-action pairs $z = (s, a) \in \mathcal{Z} = \mathcal{S} \times \mathcal{A}$, with an initial density $\rho_0^{\pi_{\theta}}(z_0) = \pi_{\theta}(a_0|s_0)\rho_0(s_0)$ and a transition probability distribution $P^{\pi_{\theta}}(z_t|z_{t-1}) = \pi_{\theta}(a_t|s_t)P(s_t|z_{t-1})$. For a time step t , we define the state-action occupancy density $P_t^{\pi_{\theta}}(z_t)$ and the discounted state-action visitation $\rho^{\pi_{\theta}}$ as,

$$P_t^{\pi_{\theta}}(z_t) = \int_{\mathcal{Z}_t} dz_0 \dots dz_{t-1} P_0^{\pi_{\theta}}(z_0) \prod_{\tau=1}^t P^{\pi_{\theta}}(z_{\tau}|z_{\tau-1}), \quad \rho^{\pi_{\theta}}(z) = \sum_{t=0}^{\infty} \gamma^t P_t^{\pi_{\theta}}(z). \quad (1)$$

We follow the standard definitions for the action-value $Q_{\pi_{\theta}}$, state-value $V_{\pi_{\theta}}$, advantage-value $A_{\pi_{\theta}}$ functions, and expected cumulative reward $J(\theta)$ of π_{θ} as,

$$Q_{\pi_{\theta}}(z_t) = \mathbb{E} \left[\sum_{\tau=0}^{\infty} \gamma^{\tau} r(z_{t+\tau}) \mid z_{t+\tau+1} \sim P^{\pi_{\theta}}(z_{t+\tau+1}|z_{t+\tau}) \right], \\ V_{\pi_{\theta}}(s_t) = \mathbb{E}_{a_t \sim \pi_{\theta}(\cdot|s_t)} [Q_{\pi_{\theta}}(z_t)], \quad A_{\pi_{\theta}}(z_t) = Q_{\pi_{\theta}}(z_t) - V_{\pi_{\theta}}(s_t), \quad J(\theta) = \mathbb{E}_{s \sim \rho_0} [V_{\pi_{\theta}}(s)]. \quad (2)$$

The policy gradient theorem (Sutton et al., 2000; Konda & Tsitsiklis, 2000) provides an analytical expression for the gradient estimate of the expected return $J(\theta)$, as:

$$\nabla_{\theta} J(\theta) = \int dz \rho^{\pi_{\theta}}(z) \nabla_{\theta} \log \pi_{\theta}(a|s) Q_{\pi_{\theta}}(z) = \mathbb{E}_{z \sim \rho^{\pi_{\theta}}} [Q_{\pi_{\theta}}(z) u(z)], \quad (3)$$

where $u(z) = \nabla_{\theta} \log \pi_{\theta}(a|s)$ is the score function. We use $\mathbb{E}_{z \sim \rho^{\pi_{\theta}}}$ and $\mathbb{E}_{\pi_{\theta}}$ interchangeably.

3 Policy Gradient Evaluation

The exact evaluation of the integral in Eq. 3 is often statistically intractable for environments with a large (or continuous) state or action space. We discuss two prominent approaches to approximate the numerical computation of the PG integral: (i) Monte-Carlo Estimation and (ii) Bayesian Quadrature.

Monte-Carlo (MC) integration approximates the integral in Eq. 3 by the finite sum:

$$\mathbf{L}_{\theta}^{MC} = \frac{1}{n} \sum_{i=1}^n Q_{\pi_{\theta}}(z_i) \mathbf{u}(z_i) = \frac{1}{n} \mathbf{U} \mathbf{Q}^{MC}, \quad (4)$$

where $\{z_i\}_{i=1}^n$ are samples from $\rho^{\pi_{\theta}}$, $\mathbf{U} = [\mathbf{u}(z_1), \dots, \mathbf{u}(z_n)]$ and $\mathbf{Q}^{MC} = [Q_{\pi_{\theta}}(z_1), \dots, Q_{\pi_{\theta}}(z_n)]^1$. In Eq. 4, $\mathbf{u}(z)$ and \mathbf{Q}^{MC} are $|\Theta|$ and n dimensional vectors, respectively, and \mathbf{U} is a $|\Theta| \times n$ dimensional matrix ($|\Theta|$ is the number of learnable parameters in the policy). MC method returns unbiased gradient estimates that eventually converge to the true gradient with more samples. However, a slow convergence rate ($n^{-1/2}$), along with high variance estimations, necessitate excessive sampling to yield reliable estimates. Nevertheless, MC methods are scalable and computationally efficient when compared to their sample-efficient alternatives (O’Hagan, 1991), making them ubiquitous in PG algorithms (Kakade, 2001; Schulman et al., 2015).

¹ $Q_{\pi_{\theta}}(z)$ is the empirical estimate of Eq. 2 under Monte-Carlo rollouts.

Bayesian quadrature (BQ) (O’Hagan, 1991) is an approach in *probabilistic numerical computing* (Hennig et al., 2015) to convert numerical integration into a Bayesian inference problem. The first step in BQ is to formulate a prior stochastic model over the integrand. By conditioning the prior model on observed samples, one can obtain the posterior model of the integrand, and through linearity of integration, the full posterior distribution over the integral. We deploy BQ to evaluate the PG integral (in Eq. 3), by placing a Gaussian process (GP) prior on the action-value function $Q_{\pi_{\theta}}$, i.e., a mean zero GP, $E[Q_{\pi_{\theta}}(z)] = 0$, with covariance function $k(z_p, z_q) = \text{Cov}[Q_{\pi_{\theta}}(z_p), Q_{\pi_{\theta}}(z_q)]$, and GP variance σ^2 . Since the transformation from $Q_{\pi_{\theta}}(z)$ to $\nabla_{\theta}J(\theta)$ happens through a linear integral operator (in Eq. 3), $\nabla_{\theta}J(\theta)$ follows a Gaussian distribution with:

$$\begin{aligned} \mathbf{L}_{\theta}^{BQ} &= E[\nabla_{\theta}J(\theta)|\mathcal{D}] = \int dz \rho^{\pi_{\theta}}(z) \mathbf{u}(z) E[Q_{\pi_{\theta}}(z)|\mathcal{D}] \\ \mathbf{C}_{\theta}^{BQ} &= \text{Cov}[\nabla_{\theta}J(\theta)|\mathcal{D}] = \int dz_1 dz_2 \rho^{\pi_{\theta}}(z_1) \rho^{\pi_{\theta}}(z_2) \mathbf{u}(z_1) \text{Cov}[Q_{\pi_{\theta}}(z_1), Q_{\pi_{\theta}}(z_2)|\mathcal{D}] \mathbf{u}(z_2)^{\top}, \end{aligned} \quad (5)$$

where the mean vector \mathbf{L}_{θ}^{BQ} is the gradient estimate and the covariance \mathbf{C}_{θ}^{BQ} is its estimation uncertainty. Following the techniques in Ghavamzadeh & Engel (2007), we use a weighted combination of universal state kernel k_s and (invariant) Fisher kernel k_f to analytically solve the integral in Eq. 5,

$$k(z_1, z_2) = c_1 k_s(s_1, s_2) + c_2 k_f(z_1, z_2), \quad \text{with } k_f(z_1, z_2) = \mathbf{u}(z_1)^{\top} \mathbf{G}^{-1} \mathbf{u}(z_2), \quad (6)$$

where c_1, c_2 are hyperparameters and \mathbf{G} is the Fisher information matrix of π_{θ} . Using the matrices,

$$\mathbf{K}_f = \mathbf{U}^{\top} \mathbf{G}^{-1} \mathbf{U}, \quad \mathbf{K} = c_1 \mathbf{K}_s + c_2 \mathbf{K}_f, \quad \mathbf{G} = \mathbb{E}_{z \sim \pi_{\theta}}[\mathbf{u}(z) \mathbf{u}(z)^{\top}] \approx \frac{1}{n} \mathbf{U} \mathbf{U}^{\top}, \quad (7)$$

we compute the mean and covariance of the gradient, (see Appendix B for the detailed derivation),

$$\mathbf{L}_{\theta}^{BQ} = c_2 \mathbf{U} (\mathbf{K} + \sigma^2 \mathbf{I})^{-1} \mathbf{Q}^{MC}, \quad \mathbf{C}_{\theta}^{BQ} = c_2 \mathbf{G} - c_2^2 \mathbf{U} (\mathbf{K} + \sigma^2 \mathbf{I})^{-1} \mathbf{U}^{\top}. \quad (8)$$

Thus, imposing a GP function approximation on the $Q_{\pi_{\theta}}$ function provides a closed-form approximation of the PG integral. In the next section, we discuss a computationally efficient deep BQ generalization of the derivation in Eq. 8, that scales to large policies and high-dimensional domains.

4 Deep Bayesian Quadrature Policy Gradient

We propose DBQPG, a novel BQ-based PG algorithm that (i) returns accurate gradient estimates, and (ii) matches the computational complexity of MC methods. In the following, we describe the components of DBQPG and the series of techniques utilized to scale it to high-dimensional settings.

Scaling BQ to large sample sizes: The complexity of estimating BQ updates (in Eq. 8) is largely influenced by the expensive computational and storage requirements of the matrix-inversion operation $(\mathbf{K} + \sigma^2 \mathbf{I})^{-1}$. We address this issue with an efficient approximation of inverse matrix-vector multiplication (MVM) using the conjugate gradient (CG) method. For an initial vector \mathbf{v} , we use CG along with iterative updates of the MVM $\mathbf{K} \mathbf{v} = c_1 \mathbf{K}_s \mathbf{v} + c_2 \mathbf{K}_f \mathbf{v}$ to quickly converge to $(\mathbf{K} + \sigma^2 \mathbf{I})^{-1} \mathbf{v}$ within machine precision.

For an efficient implementation of $\mathbf{K}_f \mathbf{v}$, we use automatic differentiation, which does not require the explicit creation or storage of the \mathbf{K}_f matrix. For computing $\mathbf{K}_s \mathbf{v}$, we deploy *structured kernel*

interpolation (SKI) (Wilson & Nickisch, 2015), a general inducing point framework for fast MVM computation. We use a set of m “inducing points”, $\{\hat{s}_i\}_{i=1}^m$, to approximate \mathbf{K}_s with a rank m matrix $\hat{\mathbf{K}}_s = \mathbf{W}\mathbf{K}_s^m\mathbf{W}^\top$, where \mathbf{K}_s^m is an $m \times m$ Gram matrix with entries $\mathbf{K}_s^m(p,q) = k_s(\hat{s}_p, \hat{s}_q)$, and \mathbf{W} is an $n \times m$ interpolation matrix. By using a local cubic interpolation (only 4 non-zero entries per row) for \mathbf{W} , we implement $\mathbf{K}_s\mathbf{v}$ operation in $\mathcal{O}(n + m^2)$ time and storage complexity.

Further, the SKI framework also provides the flexibility to select the inducing point locations for exploiting the structure of specialized GP kernels. For instance, using a product kernel along with the SKI framework can additionally leverage the Kronecker method (Saatçi, 2012) by placing the inducing points on a multidimensional grid. This combination offers an $\mathcal{O}(n + Ym^{1+1/Y})$ time and $\mathcal{O}(n + Ym^{2/Y})$ storage complexity for $\mathbf{K}_s\mathbf{v}$ operation (Y is the dimensionality of the multidimensional grid). Similarly, for stationary kernels, i.e., $k_s(x, y) = k_s(x + t, y + t) = k_s(x - y)$, along with one-dimensional inputs, the Toeplitz method (Turner, 2010) can be used by picking evenly-spaced inducing points. Since these matrices are constant along the diagonal, i.e. $\mathbf{K}_{s(x,y)} = \mathbf{K}_{s(x+1,y+1)}$, the Toeplitz method utilizes fast Fourier transform to attain an $\mathcal{O}(n + m \log m)$ time and $\mathcal{O}(n+m)$ storage for the MVM operation. Further, Toeplitz methods can be extended to multi-dimensional inputs by assuming that the kernel decomposes as a sum of one-dimensional stationary kernels along each of the input dimensions. In contrast to conventional inducing point methods that operate with $m \ll n$ inducing points, choosing a base kernel that conforms with Kronecker or Toeplitz methods enables the realization of larger m values, thereby providing a more accurate approximation of \mathbf{K}_s . We deploy these methods to provide a scalable implementation of DBQPG that matches the computation complexity of MC estimation.

Deep kernel learning: Choosing a kernel that captures a meaningful prior with respect to the target MDP is important for obtaining accurate gradient estimates and well-calibrated uncertainties (Reisinger et al., 2008). We use a deep neural network to learn the kernel bases and utilize the gradient of GP’s negative log-likelihood J_{GP} (Rasmussen & Williams, 2005) for tuning the kernel parameters ϕ , for $\zeta = \mathbf{Q}^{MC}$,

$$J_{GP}(\phi|\mathcal{D}) \propto \log |\mathbf{K}| - \zeta^\top \mathbf{K}^{-1} \zeta, \quad \nabla_\phi J_{GP} = \zeta^\top \mathbf{K}^{-1} (\nabla_\phi \mathbf{K}) \mathbf{K}^{-1} \zeta + \text{Tr}(\mathbf{K}^{-1} \nabla_\phi \mathbf{K}). \quad (9)$$

4.1 Practical DBQPG Algorithm

We choose the prior state covariance function k_s from a deep RBF kernel family, which comprises of an RBF base kernel on top of a neural network (NN) feature extractor. We choose RBF as our base kernel since (i) it is a simple exponential function with compelling theoretical properties such as infinite basis expansion and universal function approximation (Micchelli et al., 2006) and (ii) it is compatible with Kronecker and Toeplitz methods. We use SKI framework along with Toeplitz method in all our experiments for its superior computational efficiency. With a linear complexity, the practical DBQPG algorithm can efficiently estimate the gradient of a large policy network, with a few thousands of parameters, on high-dimensional continuous domains.

Besides, deep kernels combine the non-parametric flexibility of GPs with the structural properties of NNs, giving them a superior expressive power when compared to their base kernels. Our deep RBF kernel is parameterized by the lengthscale of the RBF base kernel and NN feature extractor parameters. Our implementation uses the *GPyTorch library* (Gardner et al., 2018) for optimizing the kernel parameters as it implements the gradient-based optimization in Eq. 9 using efficient matrix-matrix multiplication routines and batch conjugate gradients, effectively utilizing

the GPU hardware to dramatically accelerate kernel learning. Algorithm 1 provides an overview of the practical implementation of DBQPG, as a PG estimation subroutine.

4.2 Uncertainty Aware Policy Gradient

We propose UAPG, a novel uncertainty aware PG method that utilizes the estimation uncertainty \mathbf{C}_θ^{BQ} from DBQPG to adjust the stepsize of gradient updates. Most classical methods consider stochastic PG estimates as the true expected gradient, without accounting the estimation uncertainty in their gradient components, thus, occasionally taking large steps along the directions of high uncertainty. However, UAPG provides more reliable policy updates by lowering the stepsize along the directions with high estimation uncertainty. The UAPG updates are derived using $(\mathbf{C}_\theta^{BQ})^{-\frac{1}{2}}\mathbf{L}_\theta^{BQ}$, resulting in a gradient estimate with uniform uncertainty in all the directions. Empirically, we noticed that the spectrum of \mathbf{C}_θ^{BQ} quickly decays to a constant value, indicating that most of the principal directions have similar uncertainties (see Appendix C.4). Taking advantage of this observation, we propose a statistically and computationally efficient way of approximating the UAPG update using the rank- δ singular value decomposition (SVD) of $\mathbf{C}_\theta^{BQ} \approx \sum_{i=1}^{\delta} \mathbf{h}_i \nu_i \mathbf{h}_i^\top$ as follows:

$$\mathbf{L}_\theta^{UAPG} = \nu_\delta^{-\frac{1}{2}} (\mathbf{I} + \sum_{i=1}^{\delta} \mathbf{h}_i (\sqrt{\nu_\delta/\nu_i} - \mathbf{I}) \mathbf{h}_i^\top) \mathbf{L}_\theta^{BQ}. \quad (10)$$

The principal components (PCs) $\{\mathbf{h}_i\}_{i=1}^{\delta}$ denote the top δ directions of estimation uncertainty and the singular values $\{\nu_i\}_{i=1}^{\delta}$ denote their corresponding magnitude of uncertainty. The rank- δ decomposition of \mathbf{C}_θ^{BQ} can be efficiently computed using a fast randomized SVD algorithm (Halko et al., 2011). The UAPG update in Eq. 10 dampens the stepsize of the top δ directions of estimation uncertainty, relative to the stepsize of remaining gradient components. See Fig. 1. Thus, in comparison to DBQPG, UAPG lowers the risk of taking large steps along the directions of high uncertainty, thereby providing reliable policy updates. On the other hand, for natural gradient $\mathbf{L}_\theta^{NBQ} = \mathbf{G}^{-1}\mathbf{L}_\theta^{BQ}$, the estimation uncertainty \mathbf{C}_θ^{NBQ} is different from the uncertainty of vanilla PG, \mathbf{C}_θ^{BQ} , and is as follows:

$$\begin{aligned} \mathbf{C}_\theta^{NBQ} &= \mathbf{G}^{-1}\mathbf{C}_\theta^{BQ}\mathbf{G}^{-1} = c_2(\mathbf{G}^{-1} - c_2\mathbf{G}^{-1}\mathbf{U}(c_1\mathbf{K}_s + c_2\mathbf{K}_f + \sigma^2\mathbf{I})^{-1}\mathbf{U}^\top\mathbf{G}^{-1}) \\ &= c_2(\mathbf{G} + c_2\mathbf{U}(c_1\mathbf{K}_s + \sigma^2\mathbf{I})^{-1}\mathbf{U}^\top)^{-1}. \end{aligned} \quad (11)$$

Empirically, we observed very little variation in uncertainty along the top δ PCs of \mathbf{C}_θ^{NBQ} . Thus, instead of lowering the stepsize for the most uncertain directions of NPG (i.e., the top δ PCs of \mathbf{C}_θ^{NBQ}), we increase the step size for the most confident directions (i.e., the top δ PCs of $\mathbf{C}_\theta^{NBQ^{-1}}$):

$$\mathbf{L}_\theta^{UAPG} = \nu_\delta^{\frac{1}{2}} \left(\mathbf{I} + \sum_{i=1}^{\delta} \mathbf{h}_i (\min(\sqrt{\nu_i/\nu_\delta}, \epsilon) - \mathbf{I}) \mathbf{h}_i^\top \right) \mathbf{G}^{-1} \mathbf{L}_\theta^{BQ}, \quad \epsilon > 1 \quad (12)$$

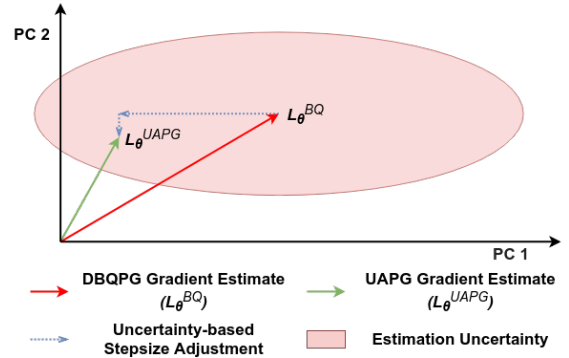


Figure 1: DBQPG and UAPG gradients along two principal components of the gradient covariance matrix.

Here, $\{\mathbf{h}_i, \nu_i\}_{i=1}^\delta$ correspond to the top δ PCs of $\mathbf{C}_\theta^{NBQ^{-1}}$, and ϵ is a hyperparameter. We replace $\sqrt{\nu_i/\nu_\delta}$ with $\min(\sqrt{\nu_i/\nu_\delta}, \epsilon)$ to avoid taking large steps along these directions, solely on the basis of their uncertainty. Interestingly, our experiments suggest that the optimal value of $c_2 \ll 1$, which makes $\mathbf{C}_\theta^{BQ} \approx c_2 \mathbf{G}$ and $\mathbf{C}_\theta^{NBQ} \approx c_2 \mathbf{G}^{-1}$. Therefore, the most uncertain gradient directions for vanilla PG approximately correspond to the most confident directions for NPG. Further, for $c_2 \ll 1$, the ideal UAPG update for both vanilla PG and NPG converges along the $\mathbf{G}^{-\frac{1}{2}} \mathbf{L}_\theta^{BQ}$ direction.

Algorithm 1 Deep Bayesian Quadrature Policy Gradient: A PG Estimation Subroutine

- 1: **DBQPG**(θ, ϕ, n, β)
 - θ : policy parameters
 - ϕ : state kernel k_s parameters ▷ feature extractor parameters + RBF’s lengthscale
 - n : sample size for PG estimation
 - β : learning rate for updating the kernel parameters
 - 2: Collect n state-action pairs from running the policy π_θ in the environment.
 - 3: Compute the MC action-value estimate \mathbf{Q}^{MC} for the n state-action pairs.
 - 4: Update kernel parameters using GP’s likelihood information.
 - 5: $\phi \leftarrow \phi + \beta \nabla_\phi J_{GP}$ ▷ Eq. 9
 - 6: Compute $\{\mathbf{h}_i, \nu_i\}_{i=1}^\delta$ using fast SVD of \mathbf{C}_θ^{BQ} (vanilla PG) or $\mathbf{C}_\theta^{NBQ^{-1}}$ (NPG) ▷ Eq. 8,11
 - 7: Policy gradient estimation:

8:	$\mathbf{L}_\theta =$	$\begin{cases} \mathbf{L}_\theta^{BQ} & \text{(DBQPG estimate of Vanilla PG)} \\ \nu_\delta^{-\frac{1}{2}} (\mathbf{I} + \sum_{i=1}^\delta \mathbf{h}_i (\sqrt{\nu_\delta/\nu_i} - \mathbf{I}) \mathbf{h}_i^\top) \mathbf{L}_\theta^{BQ} & \text{(UAPG estimate of Vanilla PG)} \\ \mathbf{G}^{-1} \mathbf{L}_\theta^{BQ} & \text{(DBQPG estimate of Natural PG)} \\ \nu_\delta^{\frac{1}{2}} (\mathbf{I} + \sum_{i=1}^\delta \mathbf{h}_i (\min(\sqrt{\nu_i/\nu_\delta}, \epsilon) - \mathbf{I}) \mathbf{h}_i^\top) \mathbf{G}^{-1} \mathbf{L}_\theta^{BQ} & \text{(UAPG estimate of Natural PG)} \end{cases}$	
----	-----------------------	---	--
 - 9: **return** ϕ, \mathbf{L}_θ ▷ updated kernel parameters, PG estimate
-

5 Experiments

We study the behaviour of BQ-based methods on MuJoCo environments, using the *mujoco-py* library of OpenAI Gym (Brockman et al., 2016). While we used MC action-value estimates \mathbf{Q}^{MC} in all our derivations, we replace them with generalized advantage estimates (Schulman et al., 2016) in our experiments as they considerably boost the performance of both MC and BQ-based methods.

Quality of Gradient Estimation: Inspired from the experimental setup of Ilyas et al. (2018), we evaluate the quality of PG estimates obtained via DBQPG and MC estimation using two metrics: (i) **gradient accuracy** or the average cosine similarity of the obtained gradient estimates with respect to the true gradient estimates (estimated from 10^6 state-action pairs) and (ii) **variance** in the gradient estimates (normalized with the norm of the mean gradient). See Fig. 2. We observe that DBQPG provides more accurate gradient estimates with a considerably lower variance. Interestingly, DBQPG and MC estimates offer nearly the same quality gradients at the start of training. However, as the training progresses, and DBQPG learns kernel bases, we observe that DBQPG returns superior quality gradient estimates. Moreover, as training progress from 0 to 150 iterations, the gradient norms of both DBQPG and MC estimates drop by a factor of 3, while

the “unnormalized” gradient variances increase by 5 folds. This indicates a drop in the signal-to-noise ratio (SNR) for gradient estimation, which also explains the drop in gradient accuracy over training time. These results motivate substituting MC with BQ-based gradient estimates in deep PG methods.

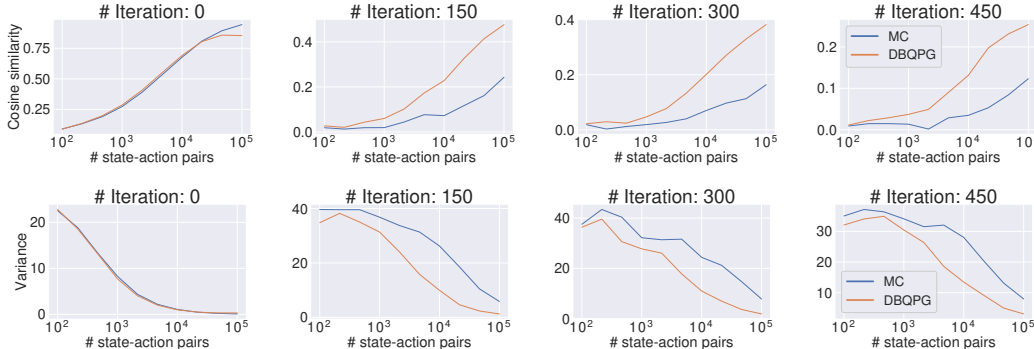


Figure 2: An empirical analysis of the quality of policy gradient estimates as a function of the state-action sample size. The experiments are conducted for 0^{th} , 150^{th} , 300^{th} , and 450^{th} iteration along the training phase of DBQPG (vanilla PG) algorithm in MuJoCo Swimmer-v2 environment. All the results have been averaged over 25 repeated gradient measurements across 100 random runs. (a) The accuracy plot results are obtained w.r.t the “true gradient”, which is computed using MC estimates of 10^6 state-action pairs. (b) The normalized variance is computed using the ratio of trace of empirical gradient covariance matrix (like Zhao et al. (2011)) and squared norm of gradient mean.

Compatibility with Deep PG Algorithms: We examine the compatibility of BQ-based methods with the following on-policy deep policy gradient algorithms: (i) Vanilla policy gradient, (ii) natural policy gradient (NPG), and (iii) trust region policy optimization (TRPO), as shown in Fig. 3. In these experiments, only the MC estimation subroutine is replaced with BQ-based methods, keeping the rest of the algorithm unchanged. We observe that DBQPG consistently outperforms MC estimation, both in final performance and sample complexity across all the deep PG algorithms. This observation resonates with our previous finding of the superior gradient quality of DBQPG estimates, and strongly advocates the use of DBQPG over MC for PG estimation whenever possible.

For UAPG, we observe a similar trend as DBQPG. The advantage of UAPG estimates is more pronounced in the vanilla PG, and NPG experiments since the performance on these algorithms is highly sensitive to the choice of learning rates, that are adaptively chosen in UAPG. UAPG adjusts the stepsize of each gradient component based on its uncertainty, resulting in a robust update in the face of uncertainty, a better sample complexity, and average return. When compared with DBQPG, we observe that UAPG performs at least as good as, if not considerably better than, DBQPG on most of the MuJoCo environments. For TRPO, we use the UAPG estimate of natural gradient to compute the step direction. Since TRPO updates are less sensitive to the learning rate, UAPG adjustment does not provide a significant improvement over DBQPG.

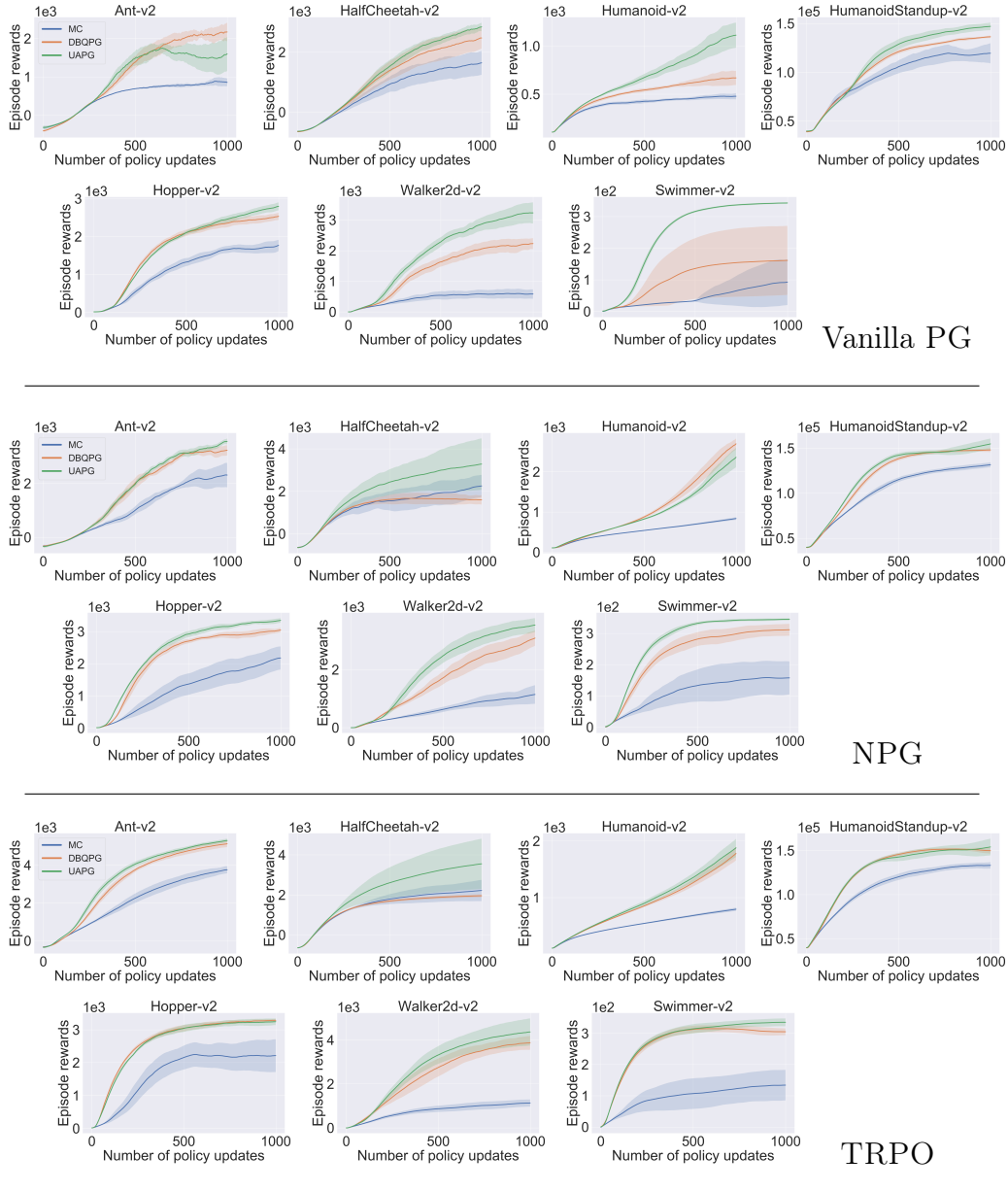


Figure 3: Comparison of BQ-based methods and MC estimation in vanilla PG, NPG, and TRPO frameworks across 7 MuJoCo environments. The agent’s performance is averaged over 10 runs.

6 Related Work

The high sample complexity in MC methods has been a long-standing problem in the PG literature (Rubinstein, 1969). Previous approaches that address this issue broadly focus on two aspects: (i) improving the quality of PG estimation using a value function approximation (Konda & Tsitsiklis, 2003), or (ii) attaining faster convergence by robustly taking larger steps in the right direction. The former class of approaches trades a tolerable level of bias for designing a lower variance PG

estimator (Sutton et al., 2000; Schulman et al., 2016; Reisinger et al., 2008). Following the latter research direction, Kakade (2001) and Kakade & Langford (2002) highlight that vanilla PG is highly dependent on the policy parameterization and instead suggest natural policy gradient (NPG), the steepest descent direction in the policy distribution space. While NPG improves over vanilla PG methods in terms of sample complexity (Peters & Schaal, 2008; Agarwal et al., 2019), it is just as vulnerable to catastrophic policy updates. Trust region policy optimization (TRPO) (Schulman et al., 2015) extends the NPG algorithm with a robust stepsize selection mechanism that guarantees monotonic improvements for expected (true) policy updates. However, the practical TRPO algorithm loses its improvement guarantees for stochastic PG estimates, thereby necessitating a large sample size for computing reliable policy updates. The advantages of these approaches, in terms of sample efficiency, are orthogonal to the benefits of DBQPG and UAPG methods. Moreover, DBQPG resembles the former class of approaches since it uses a GP function approximation to implicitly model an action-value function. Alternatively, since UAPG explicitly controls the stepsize of different gradient components based on their uncertainty, it resembles the latter class of methods.

Another line of research focuses on using Gaussian processes (GP) to directly model the PG integral (Ghavamzadeh & Engel, 2006) in closed form. This work was followed by the Bayesian Actor-Critic (BAC) algorithm (Ghavamzadeh & Engel, 2007), which exploits the MDP framework and a Bayesian critic for improving the statistical efficiency of PG estimation. Like DBQPG, BAC is a BQ-based PG method that uses a GP to approximate the action-value function. However, BAC is an online algorithm that uses Gaussian process temporal difference (GPTD) (Engel et al., 2005), a sequential kernel sparsification method, for learning the value function. While the GPTD method is more scalable than exact BQ, its relatively high $\mathcal{O}(m^2n + m^3)$ time and $\mathcal{O}(mn + m^2)$ storage complexity (m is the dictionary size, i.e., the number of inducing points) prevents it from scaling to large non-linear policies and high-dimensional continuous domains. Moreover, the online nature of the GPTD algorithm makes it incompatible with gradient-based kernel learning approaches (Wilson et al., 2014), which, based on our results, plays a crucial role in obtaining accurate PG estimates.

7 Discussion

We study the problem of estimating the gradients in PG methods when the gradient expectation is not available. In practice, an RL agent needs to come up with empirical estimates of the gradients using samples gathered through interaction with the environment. MC methods are widely used for estimating the gradients but also suffer from high variance in their estimation. We propose DBQPG, a statistically efficient approach for estimating the gradients in PG methods. We empirically study DBQPG and demonstrate its significance over MC methods. We show that DBQPG not only provides a more accurate estimation of the gradients but also maintains a significantly smaller variance in the gradient estimation. Next, we pick three principled methods from PG literature, viz., Vanilla PG, NPG, and TRPO, replace MC with DBQPG in their gradient estimation subroutine, and demonstrate significant gains in the agent’s sample complexity and average return.

To make reliable policy updates under uncertainty, one needs to estimate the uncertainty in gradient estimation, in addition to the gradient estimation itself. The proposed high dimensional Bayesian quadrature method, DBQPG, additionally provides this uncertainty along with the PG estimate. We propose UAPG, a method that takes this uncertainty into account and adjusts the gradient direction accordingly. UAPG scales the gradient components such that the stepsize along the directions with high-variance is lowered and vice versa. We further show that, using

UAPG to compute the adjusted gradient direction in Vanilla PG, NPG, and TRPO results in an extra improvement in performance. Overall, our study shows that Bayesian quadrature provides a significantly better gradient estimation, and its quantified uncertainty over gradient estimation can be used to obtain reliable policy updates.

Broader Impact

When deploying deep policy gradient (PG) algorithms for learning control policies in physical systems, sample efficiency becomes an important design criteria. In the past, numerous works have focused on improving the sample efficiency of PG estimation through variance reduction, robust stepsize selection, etc. In this paper, we propose deep Bayesian quadrature policy gradient (DBQPG), a statistically efficient policy gradient estimator that offers orthogonal benefits for improving the sample efficiency. In comparison to Monte-Carlo estimation, the default choice for PG estimation, DBQPG returns more accurate gradient estimates with much lower empirical variance. Since DBQPG is a general gradient estimation subroutine, it can directly replace Monte-Carlo estimation in most policy gradient algorithms, as already demonstrated in our paper. Therefore, we think that the DBQPG method directly benefits most policy gradient algorithms and is indirectly beneficial for several downstream reinforcement learning applications.

We also propose uncertainty aware policy gradient (UAPG), a principled approach for incorporating the uncertainty in gradient estimation (also quantified by the DBQPG method) to obtain reliable PG estimates. UAPG lowers the risk of catastrophic performance degradation with stochastic policy updates, and empirically performs at least as good as, if not better than, the DBQPG method. Hence, we believe that the UAPG method is more relevant to reinforcement learning applications with safety considerations, such as robotics.

Acknowledgements

K. Azizzadenesheli is supported in part by Raytheon and Amazon Web Service. A. Anandkumar is supported in part by Bren endowed chair, DARPA PAIHR00111890035 and LwLL grants, Raytheon, Microsoft, Google, and Adobe faculty fellowships.

References

- Agarwal, A., Kakade, S. M., Lee, J. D., and Mahajan, G. Optimality and approximation with policy gradient methods in markov decision processes. *arXiv preprint arXiv:1908.00261*, 2019.
- Bach, F. On the equivalence between kernel quadrature rules and random feature expansions. *Journal of Machine Learning Research*, 18(21):1–38, 2017. URL <http://jmlr.org/papers/v18/15-178.html>.
- Baxter, J. and Bartlett, P. L. Direct gradient-based reinforcement learning. In *2000 IEEE International Symposium on Circuits and Systems. Emerging Technologies for the 21st Century. Proceedings (IEEE Cat No. 00CH36353)*, volume 3, pp. 271–274. IEEE, 2000.

- Briol, F.-X., Oates, C., Girolami, M., and Osborne, M. A. Frank-wolfe bayesian quadrature: Probabilistic integration with theoretical guarantees. In *Advances in Neural Information Processing Systems*, pp. 1162–1170, 2015.
- Brockman, G., Cheung, V., Pettersson, L., Schneider, J., Schulman, J., Tang, J., and Zaremba, W. Openai gym, 2016.
- Duan, Y., Chen, X., Houthoofd, R., Schulman, J., and Abbeel, P. Benchmarking deep reinforcement learning for continuous control. In *Proceedings of the 33rd International Conference on International Conference on Machine Learning - Volume 48*, ICML’16, pp. 1329–1338. JMLR.org, 2016. URL <http://dl.acm.org/citation.cfm?id=3045390.3045531>.
- Engel, Y., Mannor, S., and Meir, R. Reinforcement learning with gaussian processes. In *Proceedings of the 22Nd International Conference on Machine Learning*, ICML ’05, pp. 201–208, New York, NY, USA, 2005. ACM. ISBN 1-59593-180-5. doi: 10.1145/1102351.1102377. URL <http://doi.acm.org/10.1145/1102351.1102377>.
- Gardner, J. R., Pleiss, G., Bindel, D., Weinberger, K. Q., and Wilson, A. G. Gpytorch: Blackbox matrix-matrix gaussian process inference with gpu acceleration. In *Proceedings of the 32Nd International Conference on Neural Information Processing Systems*, NIPS’18, pp. 7587–7597, USA, 2018. Curran Associates Inc. URL <http://dl.acm.org/citation.cfm?id=3327757.3327857>.
- Ghavamzadeh, M. and Engel, Y. Bayesian policy gradient algorithms. In *Proceedings of the 19th International Conference on Neural Information Processing Systems*, NIPS’06, pp. 457–464, Cambridge, MA, USA, 2006. MIT Press.
- Ghavamzadeh, M. and Engel, Y. Bayesian actor-critic algorithms. In *Proceedings of the 24th International Conference on Machine Learning*, ICML ’07, pp. 297–304, New York, NY, USA, 2007. ACM. ISBN 978-1-59593-793-3. doi: 10.1145/1273496.1273534. URL <http://doi.acm.org/10.1145/1273496.1273534>.
- Halko, N., Martinsson, P.-G., and Tropp, J. A. Finding structure with randomness: Probabilistic algorithms for constructing approximate matrix decompositions. *SIAM review*, 53(2):217–288, 2011.
- Hennig, P., Osborne, M. A., and Girolami, M. Probabilistic numerics and uncertainty in computations. *Proceedings of the Royal Society of London A: Mathematical, Physical and Engineering Sciences*, 471(2179), 2015.
- Ilyas, A., Engstrom, L., Santurkar, S., Tsipras, D., Janoos, F., Rudolph, L., and Madry, A. Are deep policy gradient algorithms truly policy gradient algorithms? *ArXiv*, abs/1811.02553, 2018.
- Kakade, S. A natural policy gradient. In *Proceedings of the 14th International Conference on Neural Information Processing Systems: Natural and Synthetic*, NIPS’01, pp. 1531–1538, Cambridge, MA, USA, 2001. MIT Press. URL <http://dl.acm.org/citation.cfm?id=2980539.2980738>.
- Kakade, S. and Langford, J. Approximately optimal approximate reinforcement learning. In *ICML*, volume 2, pp. 267–274, 2002.

- Kanagawa, M., Sriperumbudur, B. K., and Fukumizu, K. Convergence guarantees for kernel-based quadrature rules in misspecified settings. In *Advances in Neural Information Processing Systems*, pp. 3288–3296, 2016.
- Kanagawa, M., Sriperumbudur, B. K., and Fukumizu, K. Convergence analysis of deterministic kernel-based quadrature rules in misspecified settings. *Foundations of Computational Mathematics*, 20(1):155–194, 2020.
- Konda, V. R. and Tsitsiklis, J. N. Actor-critic algorithms. In Solla, S. A., Leen, T. K., and Müller, K. (eds.), *Advances in Neural Information Processing Systems 12*, pp. 1008–1014. MIT Press, 2000. URL <http://papers.nips.cc/paper/1786-actor-critic-algorithms.pdf>.
- Konda, V. R. and Tsitsiklis, J. N. On actor-critic algorithms. *SIAM J. Control Optim.*, 42(4): 1143–1166, April 2003. ISSN 0363-0129. doi: 10.1137/S0363012901385691. URL <https://doi.org/10.1137/S0363012901385691>.
- Lillicrap, T. P., Hunt, J. J., Pritzel, A., Heess, N., Erez, T., Tassa, Y., Silver, D., and Wierstra, D. Continuous control with deep reinforcement learning. *arXiv preprint arXiv:1509.02971*, 2015.
- Metropolis, N. and Ulam, S. The monte carlo method. *Journal of the American statistical association*, 44(247):335–341, 1949.
- Micchelli, C. A., Xu, Y., and Zhang, H. Universal kernels. *J. Mach. Learn. Res.*, 7:2651–2667, December 2006. ISSN 1532-4435.
- O’Hagan, A. Bayes-hermite quadrature. *Journal of Statistical Planning and Inference*, 29(3):245–260, November 1991. URL <http://www.sciencedirect.com/science/article/B6V0M-45F5GDM-53/1/6e05220bfd4a6174e890f60bb391107c>.
- Peters, J. and Schaal, S. Reinforcement learning of motor skills with policy gradients. *Neural Networks*, 21(4):682–697, May 2008.
- Puterman, M. L. *Markov decision processes: discrete stochastic dynamic programming*. John Wiley & Sons, 2014.
- Rasmussen, C. E. and Williams, C. K. I. *Gaussian Processes for Machine Learning (Adaptive Computation and Machine Learning)*. The MIT Press, 2005. ISBN 026218253X.
- Reisinger, J., Stone, P., and Miikkulainen, R. Online kernel selection for bayesian reinforcement learning. In *Proceedings of the 25th International Conference on Machine Learning, ICML ’08*, pp. 816–823, New York, NY, USA, 2008. Association for Computing Machinery. ISBN 9781605582054. doi: 10.1145/1390156.1390259. URL <https://doi.org/10.1145/1390156.1390259>.
- Rubinstein, R. Y. Some problems in monte carlo optimization. *Ph.D. thesis*, 1969.
- Saatçi, Y. *Scalable Inference for Structured Gaussian Process Models*. University of Cambridge, 2012. URL <https://books.google.co.in/books?id=9pC3oQEACAAJ>.
- Schulman, J., Levine, S., Moritz, P., Jordan, M. I., and Abbeel, P. Trust region policy optimization. In *Proceedings of the 32nd International Conference on Machine Learning (ICML)*, 2015.

- Schulman, J., Moritz, P., Levine, S., Jordan, M., and Abbeel, P. High-dimensional continuous control using generalized advantage estimation. In *Proceedings of the International Conference on Learning Representations (ICLR)*, 2016.
- Sutton, R. S., McAllester, D., Singh, S., and Mansour, Y. Policy gradient methods for reinforcement learning with function approximation. In *Proceedings of the 12th International Conference on Neural Information Processing Systems, NIPS'99*, pp. 1057–1063, Cambridge, MA, USA, 2000. MIT Press. URL <http://dl.acm.org/citation.cfm?id=3009657.3009806>.
- Todorov, E., Erez, T., and Tassa, Y. Mujoco: A physics engine for model-based control. In *2012 IEEE/RSJ International Conference on Intelligent Robots and Systems*, pp. 5026–5033. IEEE, 2012.
- Townsend, J. A new trick for calculating jacobian vector products, 2017. URL <https://j-towns.github.io/2017/06/12/A-new-trick.html>.
- Turner, R. E. *Statistical Models for Natural Sounds*. PhD thesis, Gatsby Computational Neuroscience Unit, UCL, 2010.
- Williams, R. J. Simple statistical gradient-following algorithms for connectionist reinforcement learning. *Mach. Learn.*, 8(3-4):229–256, May 1992. ISSN 0885-6125. doi: 10.1007/BF00992696. URL <https://doi.org/10.1007/BF00992696>.
- Wilson, A. G. and Nickisch, H. Kernel interpolation for scalable structured gaussian processes (kiss-gp). In *Proceedings of the 32Nd International Conference on International Conference on Machine Learning - Volume 37, ICML'15*, pp. 1775–1784. JMLR.org, 2015. URL <http://dl.acm.org/citation.cfm?id=3045118.3045307>.
- Wilson, A. G., Gilboa, E., Nehorai, A., and Cunningham, J. P. Fast kernel learning for multidimensional pattern extrapolation. In *Proceedings of the 27th International Conference on Neural Information Processing Systems - Volume 2, NIPS'14*, pp. 3626–3634, Cambridge, MA, USA, 2014. MIT Press.
- Woodbury, M. A. Inverting modified matrices. *Memorandum report*, 42(106):336, 1950.
- Zhao, T., Hachiya, H., Niu, G., and Sugiyama, M. Analysis and improvement of policy gradient estimation. In Shawe-Taylor, J., Zemel, R. S., Bartlett, P. L., Pereira, F., and Weinberger, K. Q. (eds.), *Advances in Neural Information Processing Systems 24*, pp. 262–270. Curran Associates, Inc., 2011.

A Useful Identities

Expectation of the score vector $\mathbf{u}(z) = \nabla_{\boldsymbol{\theta}} \log \pi_{\boldsymbol{\theta}}(a|s)$ under the policy distribution $\pi_{\boldsymbol{\theta}}(a|s)$ is $\mathbf{0}$:

$$\begin{aligned} \mathbb{E}_{a \sim \pi_{\boldsymbol{\theta}}(\cdot|s)} [\mathbf{u}(z)] &= \mathbb{E}_{a \sim \pi_{\boldsymbol{\theta}}(\cdot|s)} [\nabla_{\boldsymbol{\theta}} \log \pi_{\boldsymbol{\theta}}(a|s)] = \int \pi_{\boldsymbol{\theta}}(a|s) \nabla_{\boldsymbol{\theta}} \log \pi_{\boldsymbol{\theta}}(a|s) da \\ &= \int \pi_{\boldsymbol{\theta}}(a|s) \frac{\nabla_{\boldsymbol{\theta}} \pi_{\boldsymbol{\theta}}(a|s)}{\pi_{\boldsymbol{\theta}}(a|s)} da = \int \nabla_{\boldsymbol{\theta}} \pi_{\boldsymbol{\theta}}(a|s) da \\ &= \nabla_{\boldsymbol{\theta}} \left(\int \pi_{\boldsymbol{\theta}}(a|s) da \right) = \nabla_{\boldsymbol{\theta}}(1) = \mathbf{0} \end{aligned} \quad (13)$$

From Eq. 13, the expectation of the Fisher kernel k_f under the policy distribution $\pi_{\boldsymbol{\theta}}(a|s)$ is also 0:

$$\mathbb{E}_{a \sim \pi_{\boldsymbol{\theta}}(\cdot|s)} [k_f(z, z')] = \mathbb{E}_{a \sim \pi_{\boldsymbol{\theta}}(\cdot|s)} [\mathbf{u}(z)^\top \mathbf{G}^{-1} \mathbf{u}(z')] = \mathbb{E}_{a \sim \pi_{\boldsymbol{\theta}}(\cdot|s)} [\mathbf{u}(z)^\top] \mathbf{G}^{-1} \mathbf{u}(z') = 0 \quad (14)$$

B Solving Policy Gradient Integral through Bayesian Quadrature

Bayesian quadrature (BQ) (O’Hagan, 1991) provides the required machinery for estimating the numerical integration in PG (Eq. 3), by using a Gaussian process (GP) function approximation for the action-value function $Q_{\pi_{\boldsymbol{\theta}}}$. More specifically, we choose a zero mean GP, i.e., $E[Q_{\pi_{\boldsymbol{\theta}}}(z)] = 0$,² with a prior covariance function $k(z_p, z_q) = \text{Cov}[Q_{\pi_{\boldsymbol{\theta}}}(z_p), Q_{\pi_{\boldsymbol{\theta}}}(z_q)]$ and an additive Gaussian noise with variance σ^2 . One benefit of this prior is that the joint distribution over any finite number of action-values (indexed by the state-action inputs, $z \in \mathcal{Z}$) is also Gaussian:

$$\mathbf{Q}_{\pi_{\boldsymbol{\theta}}} = [Q_{\pi_{\boldsymbol{\theta}}}(z_1), \dots, Q_{\pi_{\boldsymbol{\theta}}}(z_n)] \sim \mathcal{N}(0, \mathbf{K}), \quad (15)$$

where \mathbf{K} is the Gram matrix with entries $\mathbf{K}_{p,q} = k(z_p, z_q)$. The posterior moments of $\mathbf{Q}_{\pi_{\boldsymbol{\theta}}}$ can then be obtained by using the Bayes rule to condition the GP prior on the observed samples $\mathcal{D} = \{z_i\}_{i=1}^n$ drawn from $\rho^{\pi_{\boldsymbol{\theta}}}$:

$$\begin{aligned} E[Q_{\pi_{\boldsymbol{\theta}}}(z)|\mathcal{D}] &= \mathbf{k}(z)^\top (\mathbf{K} + \sigma^2 \mathbf{I})^{-1} \mathbf{Q}^{MC}, \\ \text{Cov}[Q_{\pi_{\boldsymbol{\theta}}}(z_1), Q_{\pi_{\boldsymbol{\theta}}}(z_2)|\mathcal{D}] &= k(z_1, z_2) - \mathbf{k}(z_1)^\top (\mathbf{K} + \sigma^2 \mathbf{I})^{-1} \mathbf{k}(z_2), \\ \text{where } \mathbf{k}(z) &= [k(z_1, z), \dots, k(z_n, z)], \quad \mathbf{K} = [\mathbf{k}(z_1), \dots, \mathbf{k}(z_n)]. \end{aligned} \quad (16)$$

Since the transformation from $Q_{\pi_{\boldsymbol{\theta}}}(z)$ to $\nabla_{\boldsymbol{\theta}} J(\boldsymbol{\theta})$ happens through a linear integral operator (Eq. 3), the posterior distribution over $\nabla_{\boldsymbol{\theta}} J(\boldsymbol{\theta})$ is also Gaussian and can be computed using the posterior moments of $\mathbf{Q}_{\pi_{\boldsymbol{\theta}}}$:

$$\begin{aligned} \mathbf{L}_{\boldsymbol{\theta}}^{BQ} &= E[\nabla_{\boldsymbol{\theta}} J(\boldsymbol{\theta})|\mathcal{D}] = \int \rho^{\pi_{\boldsymbol{\theta}}}(z) \mathbf{u}(z) E[Q_{\pi_{\boldsymbol{\theta}}}(z)|\mathcal{D}] dz \\ \mathbf{C}_{\boldsymbol{\theta}}^{BQ} &= \text{Cov}[\nabla_{\boldsymbol{\theta}} J(\boldsymbol{\theta})|\mathcal{D}] = \int \rho^{\pi_{\boldsymbol{\theta}}}(z_1) \rho^{\pi_{\boldsymbol{\theta}}}(z_2) \mathbf{u}(z_1) \text{Cov}[Q_{\pi_{\boldsymbol{\theta}}}(z_1), Q_{\pi_{\boldsymbol{\theta}}}(z_2)|\mathcal{D}] \mathbf{u}(z_2)^\top dz_1 dz_2, \end{aligned} \quad (17)$$

where the posterior mean $\mathbf{L}_{\boldsymbol{\theta}}^{BQ}$ is interpreted as the policy gradient estimate and the posterior covariance $\mathbf{C}_{\boldsymbol{\theta}}^{BQ}$ quantifies the uncertainty in the policy gradient estimation. Ghavamzadeh &

²For clarity, $E[\cdot]$ denotes the mean of a Gaussian random variable, and $\mathbb{E}_{\pi_{\boldsymbol{\theta}}}[\cdot]$ denotes the expectation over samples drawn from the policy distribution.

Engel (2007) showed that the integral in Eq. 17 can be solved analytically when the GP’s prior covariance function k is the weighted combination of universal state kernel k_s and (invariant) Fisher kernel k_f :

$$k(z_1, z_2) = c_1 k_s(s_1, s_2) + c_2 k_f(z_1, z_2), \quad k_f(z_1, z_2) = \mathbf{u}(z_1)^\top \mathbf{G}^{-1} \mathbf{u}(z_2), \quad (18)$$

where c_1, c_2 are hyperparameters and \mathbf{G} is the Fisher information matrix of the policy π_θ . Some useful definitions are,

$$\mathbf{k}_f(z) = \mathbf{U}^\top \mathbf{G}^{-1} \mathbf{u}(z), \quad \mathbf{K}_f = \mathbf{U}^\top \mathbf{G}^{-1} \mathbf{U}, \quad \mathbf{K} = c_1 \mathbf{K}_s + c_2 \mathbf{K}_f, \quad \mathbf{G} = \mathbb{E}_{z \sim \pi_\theta} [\mathbf{u}(z) \mathbf{u}(z)^\top] \approx \frac{1}{n} \mathbf{U} \mathbf{U}^\top. \quad (19)$$

The closed-form expressions for the posterior moments of PG can then be obtained as follows,

$$\begin{aligned} \mathbf{L}_\theta^{BQ} &= E[\nabla_\theta J(\theta) | \mathcal{D}] = E[\mathbb{E}_{z \sim \pi_\theta} [\mathbf{u}(z) Q_{\pi_\theta}(z)] | \mathcal{D}] = \mathbb{E}_{z \sim \pi_\theta} [\mathbf{u}(z) E[Q_{\pi_\theta}(z) | \mathcal{D}]] \\ &= \int \rho^{\pi_\theta}(z) \mathbf{u}(z) E[Q_{\pi_\theta}(z) | \mathcal{D}] dz \\ &= \left(\int \rho^{\pi_\theta}(z) \mathbf{u}(z) \mathbf{k}(z)^\top dz \right) (\mathbf{K} + \sigma^2 \mathbf{I})^{-1} \mathbf{Q}^{MC} \\ &= \left(\int \rho^{\pi_\theta}(z) \mathbf{u}(z) (c_1 \mathbf{k}_s(s) + c_2 \mathbf{k}_f(z))^\top dz \right) (\mathbf{K} + \sigma^2 \mathbf{I})^{-1} \mathbf{Q}^{MC} \\ &= c_1 \left(\int \rho^{\pi_\theta}(s) \left(\int \pi_\theta(a|s) \mathbf{u}(z) da \right) \mathbf{k}_s(s)^\top ds \right) (\mathbf{K} + \sigma^2 \mathbf{I})^{-1} \mathbf{Q}^{MC} \\ &\quad + c_2 \left(\int \rho^{\pi_\theta}(z) \mathbf{u}(z) \mathbf{k}_f(z)^\top dz \right) (\mathbf{K} + \sigma^2 \mathbf{I})^{-1} \mathbf{Q}^{MC} \\ &= c_1 \left(\int \rho^{\pi_\theta}(s) (\mathbb{E}_{a \sim \pi_\theta(\cdot|s)} [\mathbf{u}(z)]) \mathbf{k}_s(s)^\top ds \right) (\mathbf{K} + \sigma^2 \mathbf{I})^{-1} \mathbf{Q}^{MC} \\ &\quad + c_2 \left(\int \rho^{\pi_\theta}(z) \mathbf{u}(z) \mathbf{k}_f(z)^\top dz \right) (\mathbf{K} + \sigma^2 \mathbf{I})^{-1} \mathbf{Q}^{MC} \\ &= c_2 \left(\int \rho^{\pi_\theta}(z) \mathbf{u}(z) \mathbf{k}_f(z)^\top dz \right) (\mathbf{K} + \sigma^2 \mathbf{I})^{-1} \mathbf{Q}^{MC} \quad (\text{from Eq. 13}^3) \\ &= c_2 \left(\int \rho^{\pi_\theta}(z) \mathbf{u}(z) \mathbf{u}(z)^\top dz \right) \mathbf{G}^{-1} \mathbf{U} (\mathbf{K} + \sigma^2 \mathbf{I})^{-1} \mathbf{Q}^{MC} \\ &= c_2 \left(\mathbb{E}_{z \sim \pi_\theta} [\mathbf{u}(z) \mathbf{u}(z)^\top] \right) \mathbf{G}^{-1} \mathbf{U} (\mathbf{K} + \sigma^2 \mathbf{I})^{-1} \mathbf{Q}^{MC} \\ &= c_2 \mathbf{G} \mathbf{G}^{-1} \mathbf{U} (c_1 \mathbf{K}_s + c_2 \mathbf{K}_f + \sigma^2 \mathbf{I})^{-1} \mathbf{Q}^{MC} \\ &= c_2 \mathbf{U} (c_1 \mathbf{K}_s + c_2 \mathbf{K}_f + \sigma^2 \mathbf{I})^{-1} \mathbf{Q}^{MC} \end{aligned} \quad (20)$$

³In Eq. 20 and 21, the following state kernel k_s terms vanish, as an extension to the identity in Eq. 13: $\mathbb{E}_{a_1 \sim \pi_\theta(\cdot|s_1)} [k_s(s_1, s_2) \mathbf{u}(z_1)] = \mathbf{0}$ and $\mathbb{E}_{a_1 \sim \pi_\theta(\cdot|s_1)} [\mathbf{u}(z_1) \mathbf{k}_s^\top(s_1)] = \mathbf{0}$.

$$\begin{aligned}
\mathbf{C}_\theta^{BQ} &= \text{Cov}(\nabla_\theta J(\theta) | \mathcal{D}) = \int dz_1 dz_2 \rho^{\pi_\theta}(z_1) \rho^{\pi_\theta}(z_2) \mathbf{u}(z_1) \text{Cov}[Q_{\pi_\theta}(z_1), Q_{\pi_\theta}(z_2) | \mathcal{D}] \mathbf{u}(z_2)^\top \\
&= \mathbb{E}_{z_1, z_2 \sim \pi_\theta} \left[\mathbf{u}(z_1) \text{Cov}[Q_{\pi_\theta}(z_1), Q_{\pi_\theta}(z_2) | \mathcal{D}] \mathbf{u}(z_2)^\top \right] \\
&= \mathbb{E}_{z_1, z_2 \sim \pi_\theta} \left[\mathbf{u}(z_1) \left(k(z_1, z_2) - \mathbf{k}(z_1)^\top (\mathbf{K} + \sigma^2 \mathbf{I})^{-1} \mathbf{k}(z_2) \right) \mathbf{u}(z_2)^\top \right] \\
&= \mathbb{E}_{z_1, z_2 \sim \pi_\theta} \left[\mathbf{u}(z_1) \left(c_1 k_s(s_1, s_2) + c_2 k_f(z_1, z_2) - \mathbf{k}(z_1)^\top (\mathbf{K} + \sigma^2 \mathbf{I})^{-1} \mathbf{k}(z_2) \right) \mathbf{u}(z_2)^\top \right] \\
&= \mathbb{E}_{z_1, z_2 \sim \pi_\theta} \left[\mathbf{u}(z_1) \left(c_2 k_f(z_1, z_2) - (c_1 \mathbf{k}_s(s_1) + c_2 \mathbf{k}_f(z_1))^\top (\mathbf{K} + \sigma^2 \mathbf{I})^{-1} \mathbf{k}(z_2) \right) \mathbf{u}(z_2)^\top \right] \\
&= \mathbb{E}_{z_1, z_2 \sim \pi_\theta} \left[\mathbf{u}(z_1) \left(c_2 k_f(z_1, z_2) - c_2 \mathbf{k}_f(z_1)^\top (\mathbf{K} + \sigma^2 \mathbf{I})^{-1} (c_1 \mathbf{k}_s(s_2) + c_2 \mathbf{k}_f(z_2)) \right) \mathbf{u}(z_2)^\top \right] \\
&= \mathbb{E}_{z_1, z_2 \sim \pi_\theta} \left[\mathbf{u}(z_1) \left(c_2 k_f(z_1, z_2) - c_2^2 \mathbf{k}_f(z_1)^\top (\mathbf{K} + \sigma^2 \mathbf{I})^{-1} \mathbf{k}_f(z_2) \right) \mathbf{u}(z_2)^\top \right] \\
&= \mathbb{E}_{z_1, z_2 \sim \pi_\theta} \left[\mathbf{u}(z_1) \mathbf{u}(z_1)^\top \left(c_2 \mathbf{G}^{-1} - c_2^2 \mathbf{G}^{-1} \mathbf{U} (\mathbf{K} + \sigma^2 \mathbf{I})^{-1} \mathbf{U}^\top \mathbf{G}^{-1} \right) \mathbf{u}(z_2) \mathbf{u}(z_2)^\top \right] \\
&= \mathbb{E}_{z_1 \sim \pi_\theta} [\mathbf{u}(z_1) \mathbf{u}(z_1)^\top] \left(c_2 \mathbf{G}^{-1} - c_2^2 \mathbf{G}^{-1} \mathbf{U} (\mathbf{K} + \sigma^2 \mathbf{I})^{-1} \mathbf{U}^\top \mathbf{G}^{-1} \right) \mathbb{E}_{z_2 \sim \pi_\theta} [\mathbf{u}(z_2) \mathbf{u}(z_2)^\top] \\
&= \mathbf{G} \left(c_2 \mathbf{G}^{-1} - c_2^2 \mathbf{G}^{-1} \mathbf{U} (\mathbf{K} + \sigma^2 \mathbf{I})^{-1} \mathbf{U}^\top \mathbf{G}^{-1} \right) \mathbf{G} \\
&= c_2 \mathbf{G} - c_2^2 \mathbf{U} (c_1 \mathbf{K}_s + c_2 \mathbf{K}_f + \sigma^2 \mathbf{I})^{-1} \mathbf{U}^\top
\end{aligned} \tag{21}$$

Furthermore, the inverse of \mathbf{C}_θ^{BQ} can also be analytically computed using the Woodbury matrix identity (Woodbury, 1950):

$$\begin{aligned}
\left(\mathbf{C}_\theta^{BQ} \right)^{-1} &= \left(c_2 \mathbf{G} - c_2^2 \mathbf{U} (c_1 \mathbf{K}_s + c_2 \mathbf{K}_f + \sigma^2 \mathbf{I})^{-1} \mathbf{U}^\top \right)^{-1} \\
&= \frac{1}{c_2} \mathbf{G}^{-1} + \mathbf{G}^{-1} \mathbf{U} \left(c_1 \mathbf{K}_s + c_2 \mathbf{K}_f + \sigma^2 \mathbf{I} - c_2 \mathbf{U}^\top \mathbf{G}^{-1} \mathbf{U} \right)^{-1} \mathbf{U}^\top \mathbf{G}^{-1} \\
&= \frac{1}{c_2} \mathbf{G}^{-1} + \mathbf{G}^{-1} \mathbf{U} (c_1 \mathbf{K}_s + \sigma^2 \mathbf{I})^{-1} \mathbf{U}^\top \mathbf{G}^{-1}
\end{aligned} \tag{22}$$

Thus, by choosing the overall kernel as a weighted combination of the Fisher kernel k_f and an arbitrary state kernel k_s , the BQ approach has a closed-form expression for the gradient mean \mathbf{L}_θ^{BQ} and its estimation uncertainty \mathbf{C}_θ^{BQ} (gradient covariance).

C Scaling BQ to High-Dimensional Settings

In comparison to Monte-Carlo methods, BQ approaches have several appealing properties, such as a strictly faster convergence rate (Briol et al., 2015; Kanagawa et al., 2016, 2020; Bach, 2017) and a logical propagation of numerical uncertainty from the action-value Q_{π_θ} function space to the posterior distribution over the policy gradient. However, the complexity of estimating BQ’s posterior moments, \mathbf{L}_θ^{BQ} and \mathbf{C}_θ^{BQ} , is largely influenced by the computationally expensive matrix-inversion operation $(\mathbf{K} + \sigma^2 \mathbf{I})^{-1}$. The storage and inversion of this $n \times n$ sized matrix (n is the sample size) is computationally infeasible in all but the smallest and simplest of continuous domains. In the

following, we provide a detailed description of the DBQPG method (Sec. 4 in the main paper) that allows us to scale BQ to high-dimensional settings, while retaining the superior statistical efficiency over MC methods.

Algorithm 2 Conjugate Gradient Algorithm

```

1: CG(MVM,  $\mathbf{v}$ ,  $\varphi$ )
   •  $\mathbf{v}$ : The vector for which  $M^{-1}\mathbf{v}$  needs to be computed.
   • MVM( $\mathbf{v}$ ): A sub-routine that takes a vector  $\mathbf{v}$  and returns  $M\mathbf{v}$ .
   •  $\varphi$ : Terminates the routine when the residual is lower than  $\varphi$ .
2:  $\mathbf{x}_0 = \mathbf{0}$  ▷ Initial guess of the solution.
3:  $\mathbf{r}_0 = \mathbf{v} - \text{MVM}(\mathbf{x}_0)$  ▷ Residual for the initial solution.
4: if  $\mathbf{r}_0 < \varphi$  then
5:   return  $\mathbf{x}_0, \mathbf{r}_0$ 
6: end if
7:  $\mathbf{p}_0 = \mathbf{r}_0$  ▷ Initial search direction.
8:  $i = 0$  ▷ Iteration counter.
9: repeat
10:   $\chi_i = \mathbf{r}_i \mathbf{r}_i^\top / \mathbf{p}_i^\top \text{MVM}(\mathbf{p}_i)$ 
11:   $\mathbf{x}_{i+1} = \mathbf{x}_i + \chi_i \mathbf{p}_i$ 
12:   $\mathbf{r}_{i+1} = \mathbf{r}_i - \chi_i \text{MVM}(\mathbf{p}_i)$ 
13:   $\psi_i = \mathbf{r}_{i+1}^\top \mathbf{r}_{i+1} / \mathbf{r}_i^\top \mathbf{r}_i$ 
14:   $\mathbf{p}_{i+1} = \mathbf{r}_{i+1} + \psi_i \mathbf{p}_i$ 
15:   $i = i + 1$ 
16: until  $\mathbf{r}_{i+1} < \varphi$ 
17: return  $\mathbf{x}_{i+1}, \mathbf{r}_{i+1}$ 

```

We first describe the conjugate gradient (CG) algorithm in Algorithm 2, which provides the foundation for scaling BQ to large sample sizes. More precisely, we utilize the CG algorithm to replace an expensive matrix-inversion operation with an efficient approximation of inverse matrix-vector multiplication (MVM). Using the conjugate gradient (CG) algorithm, an inverse MVM operation can be computed implicitly, i.e., without the explicit storage or inversion of the matrix, by simply following iterative routines of efficient matrix-vector multiplications (MVMs) (see Algorithm 2). For a given vector \mathbf{v} , the computational complexity for solving $(\mathbf{K} + \sigma^2 \mathbf{I})^{-1} \mathbf{v}$ with p iterations of CG is $\mathcal{O}(p\mathcal{M})$, where \mathcal{M} is the computational complexity associated with the MVM computation $\mathbf{K}\mathbf{v}$. One of the appealing properties of the CG algorithm is that a convergence, within machine precision, can be obtained using only a small number $p \ll n$ of iterations. However, naively computing $\mathbf{K}\mathbf{v} = c_1 \mathbf{K}_s \mathbf{v} + c_2 \mathbf{K}_f \mathbf{v}$ still has a prohibitive $\mathcal{O}(n^2)$ time and storage complexity. We propose separate strategies for efficiently computing $\mathbf{K}_s \mathbf{v}$ and $\mathbf{K}_f \mathbf{v}$.

C.1 Efficient MVM Computation with Fisher Covariance Matrix

The Fisher covariance matrix \mathbf{K}_f of a policy π_θ can be factorized as the product of three matrices, $\mathbf{U}^\top \mathbf{G}^{-1} \mathbf{U}$, which enables us to efficiently implement $\mathbf{K}_f \mathbf{v}$ in two distinct ways.

Approach 1 (slow): One way is to look at the \mathbf{U} matrix as the transpose of Jacobian of the log-probabilities and \mathbf{G} matrix as the hessian of the KL divergence, with respect to policy

parameters θ . As a result, $\mathbf{K}_f \mathbf{v}$ can be directly computed sequentially using three MVM routines: (i) a vector-Jacobian product (vJp) involving the \mathbf{U} matrix, followed by (ii) an inverse-Hessian-vector product involving the \mathbf{G} matrix, and finally (iii) a Jacobian-vector product (Jvp) involving the \mathbf{U} matrix.

$$\mathbf{K}_f \mathbf{v} = \left(\mathbf{U}^\top (\mathbf{G}^{-1} (\mathbf{U} \mathbf{v})) \right) = \left(\frac{\partial \mathcal{L}}{\partial \theta} \left(\mathbf{G}^{-1} \left(\left(\frac{\partial \mathcal{L}}{\partial \theta} \right)^\top \mathbf{v} \right) \right) \right), \quad (23)$$

where $\mathcal{L} = [\log \pi_\theta(a_1|s_1), \dots, \log \pi_\theta(a_n|s_n)]$, $(s_i, a_i) \sim \pi_\theta \forall i \in [1, n]$.

The vector-Jacobian Product vJp can be straight-forwardly computed using regular reverse-mode automatic differentiation (AD) as follows, $\left(\frac{\partial \mathcal{L}}{\partial \theta} \right)^\top \mathbf{v} = \frac{\partial (\mathcal{L}^\top \mathbf{v})}{\partial \theta}$. Most standard AD and neural network packages also support Hessian-vector product Hvp , and subsequently, the CG algorithm can be used for computing the inverse- Hvp (a.k.a the KL divergence trick used in TRPO (Schulman et al., 2015)). On the other hand, a Jvp can be computed using the trick suggested in Appendix D. While this procedure offers a linear complexity for estimating $\mathbf{K}_f \mathbf{v}$, in practice, the numerous backward calls (reverse-mode automatic differentiation) noticeably slows down the MVM operation.

Approach 2 (fast): It can be seen that the $n \times n$ dimensional matrix $\mathbf{K}_f = \mathbf{U}^\top \mathbf{G}^{-1} \mathbf{U}$ has a rank $|\Theta| < n$ (since \mathbf{U} has the dimensions $|\Theta| \times n$). To efficiently compute $\mathbf{K}_f \mathbf{v}$, it helps to first visualize the \mathbf{U} matrix in terms of its full singular value decomposition (SVD), $\mathbf{U} = \mathbf{P} \mathbf{\Lambda} \mathbf{R}^\top$, where \mathbf{P} and \mathbf{R} are orthogonal matrices with dimensions $|\Theta| \times |\Theta|$ and $n \times |\Theta|$ respectively, and $\mathbf{\Lambda}$ is an $|\Theta| \times |\Theta|$ diagonal matrix of singular values. Consequently, the expressions for \mathbf{G} and \mathbf{K}_f can be simplified as follows:

$$\begin{aligned} \mathbf{G} &= \frac{1}{n} \mathbf{U} \mathbf{U}^\top = \frac{1}{n} \mathbf{P} \mathbf{\Lambda}^2 \mathbf{P}^\top, \\ \mathbf{K}_f &= \mathbf{U}^\top \mathbf{G}^{-1} \mathbf{U} = n \mathbf{R} \mathbf{\Lambda} \mathbf{P}^\top \left(\mathbf{P} \mathbf{\Lambda}^{-2} \mathbf{P}^\top \right) \mathbf{P} \mathbf{\Lambda} \mathbf{R}^\top = n \mathbf{R} \mathbf{R}^\top. \end{aligned} \quad (24)$$

In practice, we avoid the computational overhead of a full SVD by using fast randomized SVD (Halko et al., 2011) to compute the rank $\delta \ll |\Theta|$ approximations for \mathbf{P} , $\mathbf{\Lambda}$ and \mathbf{R} , i.e. $|\Theta| \times \delta$, $\delta \times \delta$ and $n \times \delta$ dimensional matrices respectively. Further, the fast SVD of the \mathbf{U} matrix can be computed using an iterative routine of implicit MVM computations, thus, avoiding the explicit formation and storage of the \mathbf{U} matrix at any point of time. Interestingly, it can be seen that the rank δ approximation of the \mathbf{K}_f matrix is equivalent to a linear kernel of dimensions δ , with inputs being the rows in $\sqrt{n} \mathbf{R}$ matrix. The implicit low-rank nature of the linear kernel allows for efficient MVM computation for \mathbf{K}_f in $\mathcal{O}(n\delta)$ time and space complexity.

C.2 Efficient MVM Computation with State Covariance Matrix

Since the choice of the state kernel k_s is arbitrary, we rely on *structured kernel interpolation (SKI)* (Wilson & Nickisch, 2015), a general inducing point framework for fast MVM computation. Using m inducing points $\{\hat{s}_i\}_{i=1}^m$, SKI replaces the \mathbf{K}_s matrix with a rank m approximation $\hat{\mathbf{K}}_s = \mathbf{W} \mathbf{K}_s^m \mathbf{W}^\top$, where \mathbf{K}_s^m is an $m \times m$ Gram matrix with entries $\mathbf{K}_s^m(p, q) = k_s(\hat{s}_p, \hat{s}_q)$, and \mathbf{W} is an $n \times m$ interpolation matrix. Thus, $\hat{\mathbf{K}}_s \mathbf{v}$ can be computed using three successive MVMs: (i) an MVM with \mathbf{W}^\top , followed by (ii) an MVM with \mathbf{K}_s^m , and finally (iii) an MVM with \mathbf{W} . To compute the MVM with \mathbf{W} matrix in linear time, Wilson & Nickisch (2015) suggests a local cubic interpolation

(only 4 non-zero entries per row). Thus, even a naive $\mathcal{O}(m^2)$ implementation of an MVM with \mathbf{K}_s^m substantially reduces the complexity of $\hat{\mathbf{K}}_s \mathbf{v}$ to $\mathcal{O}(n + m^2)$ time and storage. Additionally, the SKI framework allows choosing the inducing point locations to further exploit the structure in GP’s kernel functions, e.g., (i) using the Kronecker method (Saatçi, 2012) with a product kernel for an $\mathcal{O}(n + Ym^{1+1/Y})$ time and $\mathcal{O}(n + Ym^{2/Y})$ storage complexity, or (ii) the Topelitz method (Turner, 2010) with a stationary kernel for an $\mathcal{O}(n + m \log m)$ time and $\mathcal{O}(n + m)$ storage complexity.

C.3 Practical DBQPG Algorithm

In addition to the details from Sec. 4.1 (main paper), we provide a step-by-step explanation for efficiently estimating the PG mean \mathbf{L}_θ^{BQ} . In our practical implementation, we replace the action-value estimates \mathbf{Q}^{MC} with the generalized advantage estimates \mathbf{A}^{GAE} for a better sample complexity. The first step is to compute the n dimensional \mathbf{A}^{GAE} vector by following Schulman et al. (2016). The next step is to compute $\alpha = (c_1 \mathbf{K}_s + c_2 \mathbf{K}_f + \sigma^2 \mathbf{I})^{-1} \mathbf{A}^{GAE}$ using the conjugate gradient algorithm (Algorithm 2), and efficient $\mathbf{K}_f \mathbf{A}^{GAE}$ (Appendix C.1) and $\mathbf{K}_s \mathbf{A}^{GAE}$ (Appendix C.2) operations. Finally, $\mathbf{L}_\theta^{BQ} = \mathbf{U} \alpha$ can be computed using a vJp involving the \mathbf{U} matrix. For natural gradient algorithms (e.g. NPG and TRPO), we perform an additional MVM routine which uses the CG algorithm along with the Hvp of the KL divergence (similar to the Hvp computation in C.1 Approach 1 and Schulman et al. (2015)).

C.4 Practical UAPG Algorithm

Ideally, the UAPG update has to be computed as follows $\mathbf{L}_\theta^{UAPG} = (\mathbf{C}_\theta^{BQ})^{-\frac{1}{2}} \mathbf{L}_\theta^{BQ}$. By expressing the estimation uncertainty \mathbf{C}_θ^{BQ} in terms of its full SVD, $\mathbf{C}_\theta^{BQ} = \sum_{i=1}^{|\Theta|} \mathbf{h}_i \nu_i \mathbf{h}_i^\top$, the UAPG update can equivalently be expressed as follows,

$$\mathbf{L}_\theta^{UAPG} = \sum_{i=1}^{|\Theta|} \left(\mathbf{h}_i \left(\sqrt{\frac{1}{\nu_i}} \right) \mathbf{h}_i^\top \right) \mathbf{L}_\theta^{BQ} \quad (25)$$

However, the empirical estimate of $\mathbf{G} = \frac{1}{n} \mathbf{U} \mathbf{U}^\top$ is often a low-rank matrix ($\text{rank} \ll |\Theta|$), since a practically-feasible sample size is generally inadequate for the full rank computation in high-dimensional settings. To improve the numerical stability of computations involving inverse of such low-rank matrices (e.g. natural gradient computation, Eq. 25, etc.), one can (i) unreasonably increase the sample size n for obtaining a full rank estimate (statistically infeasible) or (ii) add a small scalar matrix (practical approach). In our implementation, we add a $0.1 \mathbf{I}$ term to the empirical estimation of the fisher information matrix for improving the stability of matrix inversion (similar to the official TRPO implementation (Schulman et al., 2015)).

From another perspective, the exact computation of Eq. 25 is computationally infeasible for large policy networks (> 1000 learnable parameters). Due to the additional $0.1 \mathbf{I}$ term, the spectrum of \mathbf{C}_θ^{BQ} quickly decays to 0.1 and no further (see Fig. 4). Taking advantage of this observation, we propose a rank $\delta \ll |\Theta|$ SVD approximation for \mathbf{C}_θ^{BQ} for computing an approximate UAPG update \mathbf{L}_θ^{UAPG} that only considers the δ singular values that are greater than 0.1,

$$\mathbf{L}_\theta^{UAPG} = \nu_\delta^{-\frac{1}{2}} (\mathbf{I} + \sum_{i=1}^{\delta} \mathbf{h}_i (\sqrt{\nu_\delta / \nu_i} - \mathbf{I}) \mathbf{h}_i^\top) \mathbf{L}_\theta^{BQ}. \quad (26)$$

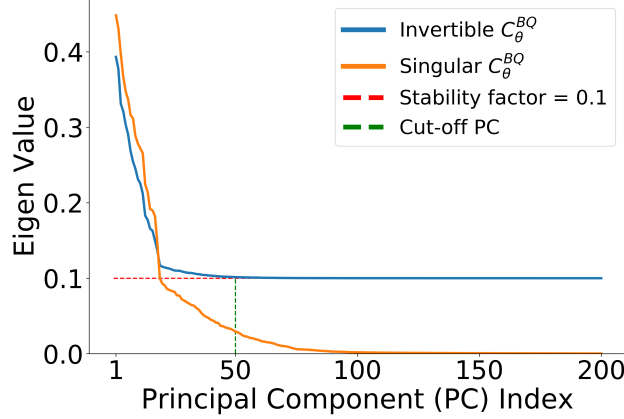


Figure 4: Top 200 principal components of \mathbf{C}_θ^{BQ} along with their respective singular values at the 0^{th} iteration of the Walker2d-v2 environment.

Further, this equation can be efficiently computed through fast randomized SVD (Halko et al., 2011). For NPG and TRPO algorithms that follow a natural gradient update $\mathbf{L}_\theta^{NBQ} = \mathbf{G}^{-1} \mathbf{L}_\theta^{BQ}$, the estimation uncertainty \mathbf{C}_θ^{NBQ} is,

$$\begin{aligned}
 \mathbf{C}_\theta^{NBQ} &= \mathbf{G}^{-1} \mathbf{C}_\theta^{BQ} \mathbf{G}^{-1} \\
 &= c_2 (\mathbf{G}^{-1} - c_2 \mathbf{G}^{-1} \mathbf{U} (c_1 \mathbf{K}_s + c_2 \mathbf{K}_f + \sigma^2 \mathbf{I})^{-1} \mathbf{U}^\top \mathbf{G}^{-1}) \\
 &= c_2 (\mathbf{G} + c_2 \mathbf{U} (c_1 \mathbf{K}_s + \sigma^2 \mathbf{I})^{-1} \mathbf{U}^\top)^{-1}, \tag{27}
 \end{aligned}$$

and the ideal UAPG update is $\mathbf{L}_\theta^{UAPG} = (\mathbf{C}_\theta^{NBQ})^{-\frac{1}{2}} \mathbf{G}^{-1} \mathbf{L}_\theta^{BQ}$. However, the low-rank nature of empirical \mathbf{G} and \mathbf{U} matrices, along with the $0.1\mathbf{I}$ term, causes the singular values to be close to 10 for all but the bottom δ singular values, which correspond to the confident directions of natural gradient estimation. Thus, these bottom δ singular values have a value lower than 10. To obtain the natural gradient UAPG update, we perform a rank $\delta \ll |\Theta|$ SVD approximation for $\mathbf{C}_\theta^{NBQ^{-1}}$, that computes the top δ singular values of $\mathbf{C}_\theta^{NBQ^{-1}}$, which are the same as the bottom δ PCs of \mathbf{C}_θ^{NBQ} ,

$$\mathbf{L}_\theta^{UAPG} = \nu_\delta^{\frac{1}{2}} \left(\mathbf{I} + \sum_{i=1}^{\delta} \mathbf{h}_i (\min(\sqrt{\nu_i/\nu_\delta}, \epsilon) - \mathbf{I}) \mathbf{h}_i^\top \right) \mathbf{G}^{-1} \mathbf{L}_\theta^{BQ}, \quad \epsilon > 1 \tag{28}$$

Further, we replace $\sqrt{\nu_i/\nu_\delta}$ with $\min(\sqrt{\nu_i/\nu_\delta}, \epsilon)$ to avoid taking large steps along these directions, solely on the basis of their uncertainty.

D Jacobian-Vector Product using Reverse-Mode Automatic Differentiation

While a vector-Jacobian Product (vJp) can be straight-forwardly computed using regular reverse-mode automatic differentiation, it is non-trivial to efficiently compute a Jacobian-vector Product

(*Jvp*). Prior approaches either calculate the entire Jacobian matrix which cannot be extended to high-dimensional problems or use a forward-mode automatic differentiation which is not supported in most automatic differentiation and neural network packages. Instead, we follow a recently introduced trick (Townsend, 2017) to estimate the *Jvp* using only two successive *vJp* operations, using only reverse-mode automatic differentiation:

$$\begin{aligned} vjp(\mathcal{L})(\mathbf{w}_{temp}, \boldsymbol{\theta}) &= (\mathbf{w}_{temp})^\top \frac{\partial \mathcal{L}}{\partial \boldsymbol{\theta}}, \\ jvp(\mathcal{L})(\mathbf{v}, \boldsymbol{\theta}) &= \frac{\partial \mathcal{L}}{\partial \boldsymbol{\theta}} \mathbf{v} = \left[vjp \left([vjp(\mathcal{L})(\mathbf{w}_{temp}, \boldsymbol{\theta})]^\top \right) (\mathbf{v}, \mathbf{w}_{temp}) \right]^\top. \end{aligned} \quad (29)$$

E Interesting Properties of BQ-based Methods

E.1 Posterior Moments of the Value Functions

The posterior moments of the action-value function Q_{π_θ} (see Eq. 16), along with the identities in Eq. 13 and 14 can be used to derive the expressions for the posterior moments of the state-value function V_{π_θ} and the advantage function A_{π_θ} as follows:

$$\begin{aligned} E[V_{\pi_\theta}(s)|\mathcal{D}] &= \mathbb{E}_{a \sim \pi_\theta(\cdot|s)} [E[Q_{\pi_\theta}(z)|\mathcal{D}]] = \mathbb{E}_{a \sim \pi_\theta(\cdot|s)} \left[\mathbf{k}(z)^\top \right] (\mathbf{K} + \sigma^2 \mathbf{I})^{-1} \mathbf{Q}^{MC} \\ &= \mathbb{E}_{a \sim \pi_\theta(\cdot|s)} \left[(c_1 \mathbf{k}_s(s) + c_2 \mathbf{k}_f(z))^\top \right] (\mathbf{K} + \sigma^2 \mathbf{I})^{-1} \mathbf{Q}^{MC} \\ &= (c_1 \mathbf{k}_s(s) + c_2 \mathbb{E}_{a \sim \pi_\theta(\cdot|s)} [\mathbf{k}_f(z)])^\top (\mathbf{K} + \sigma^2 \mathbf{I})^{-1} \mathbf{Q}^{MC} \\ &= c_1 \mathbf{k}_s(s)^\top (\mathbf{K} + \sigma^2 \mathbf{I})^{-1} \mathbf{Q}^{MC} \end{aligned} \quad (30)$$

$$\begin{aligned} E[A_{\pi_\theta}(z)|\mathcal{D}] &= E[(Q_{\pi_\theta}(z) - V_{\pi_\theta}(s))|\mathcal{D}] = E[Q_{\pi_\theta}(z)|\mathcal{D}] - E[V_{\pi_\theta}(s)|\mathcal{D}] \\ &= (\mathbf{k}(z) - c_1 \mathbf{k}_s(s))^\top (c_1 \mathbf{K}_s + c_2 \mathbf{K}_f + \sigma^2 \mathbf{I})^{-1} \mathbf{Q}^{MC} \\ &= c_2 \mathbf{k}_f(z)^\top (c_1 \mathbf{K}_s + c_2 \mathbf{K}_f + \sigma^2 \mathbf{I})^{-1} \mathbf{Q}^{MC} \end{aligned} \quad (31)$$

$$\begin{aligned} \text{Cov}[V_{\pi_\theta}(s_1), Q_{\pi_\theta}(z_2)|\mathcal{D}] &= \mathbb{E}_{a_1 \sim \pi_\theta(\cdot|s_1)} [\text{Cov}[Q_{\pi_\theta}(z_1), Q_{\pi_\theta}(z_2)|\mathcal{D}]], \\ &= \mathbb{E}_{a_1 \sim \pi_\theta(\cdot|s_1)} \left[k(z_1, z_2) - \mathbf{k}(z_1)^\top (\mathbf{K} + \sigma^2 \mathbf{I})^{-1} \mathbf{k}(z_2) \right] \\ &= c_1 k_s(s_1, s_2) - c_1 \mathbf{k}_s(s_1)^\top (\mathbf{K} + \sigma^2 \mathbf{I})^{-1} \mathbf{k}(z_2) \end{aligned} \quad (32)$$

$$\begin{aligned} \text{Cov}[V_{\pi_\theta}(s_1), V_{\pi_\theta}(s_2)|\mathcal{D}] &= \mathbb{E}_{a_2 \sim \pi_\theta(\cdot|s_2)} [\text{Cov}[V_{\pi_\theta}(s_1), Q_{\pi_\theta}(z_2)|\mathcal{D}]] \\ &= c_1 k_s(s_1, s_2) - c_1 \mathbf{k}_s(s_1)^\top (\mathbf{K} + \sigma^2 \mathbf{I})^{-1} \mathbb{E}_{a_2 \sim \pi_\theta(\cdot|s_2)} [\mathbf{k}(z_2)] \\ &= c_1 k_s(s_1, s_2) - c_1^2 \mathbf{k}_s(s_1)^\top (\mathbf{K} + \sigma^2 \mathbf{I})^{-1} \mathbf{k}_s(s_2) \end{aligned} \quad (33)$$

$$\begin{aligned} \text{Cov}[A_{\pi_\theta}(z_1), Q_{\pi_\theta}(z_2)|\mathcal{D}] &= \text{Cov}[Q_{\pi_\theta}(z_1) - V_{\pi_\theta}(s_1), Q_{\pi_\theta}(z_2)|\mathcal{D}] \\ &= c_2 k_f(z_1, z_2) - c_2 \mathbf{k}_f(z_1)^\top (\mathbf{K} + \sigma^2 \mathbf{I})^{-1} \mathbf{k}(z_2) \end{aligned} \quad (34)$$

$$\begin{aligned}
\text{Cov}[A_{\pi_\theta}(z_1), A_{\pi_\theta}(z_2)|\mathcal{D}] &= \text{Cov}[A_{\pi_\theta}(z_1), Q_{\pi_\theta}(z_2)|\mathcal{D}] - \mathbb{E}_{a_2 \sim \pi_\theta(\cdot|s_2)}[\text{Cov}[A_{\pi_\theta}(z_1), Q_{\pi_\theta}(z_2)|\mathcal{D}]] \\
&= c_2 k_f(z_1, z_2) - c_2^2 \mathbf{k}_f(z_1)^\top (\mathbf{K} + \sigma^2 \mathbf{I})^{-1} \mathbf{k}_f(z_2).
\end{aligned} \tag{35}$$

Therefore, by choosing the overall kernel as a weighted combination of the Fisher kernel k_f and an arbitrary state kernel k_s , k_f implicitly models the advantage value function A_{π_θ} while k_s models the state value function V_{π_θ} . In other words, choosing $c_1 = 0$ and $c_2 = 0$ nullifies the posterior moments of V_{π_θ} and A_{π_θ} respectively.

E.2 MC Estimation is a Degenerate Case of BQ

When the state kernel is set to 0, i.e. $c_1 = 0$, we demonstrate that the BQ's posterior mean degenerates to the Monte-Carlo mean estimate (Eq. 4 in the main paper). Further, the action-value GP's prior and the posterior covariance matrices become the scalar multiples of the Fisher information matrix (\mathbf{G}).

$$\begin{aligned}
\mathbf{L}_\theta^{BQ}|_{c_1=0} &= c_2 \mathbf{U} (0 * \mathbf{K}_s + c_2 \mathbf{K}_f + \sigma^2 \mathbf{I})^{-1} \mathbf{Q}^{MC} \\
&= c_2 \mathbf{U} (c_2 \mathbf{K}_f + \sigma^2 \mathbf{I})^{-1} \mathbf{Q}^{MC} \\
&= c_2 \mathbf{U} (c_2 \mathbf{U}^\top \mathbf{G}^{-1} \mathbf{U} + \sigma^2 \mathbf{I})^{-1} \mathbf{Q}^{MC} \\
&= c_2 \mathbf{U} \left(\frac{1}{\sigma^2} \mathbf{I} - \frac{c_2}{\sigma^4} \mathbf{U}^\top \left(\mathbf{G} + \frac{c_2}{\sigma^2} \mathbf{U} \mathbf{U}^\top \right)^{-1} \mathbf{U} \right) \mathbf{Q}^{MC} \\
&= \frac{c_2}{\sigma^2} \mathbf{U} \left(\mathbf{I} - \frac{c_2}{\sigma^2} \mathbf{U}^\top \left(\mathbf{G} + \frac{c_2 M}{\sigma^2} \mathbf{G} \right)^{-1} \mathbf{U} \right) \mathbf{Q}^{MC} \\
&= \frac{c_2}{\sigma^2} \mathbf{U} \left(\mathbf{I} - \frac{c_2}{(\sigma^2 + c_2 M)} \mathbf{U}^\top \mathbf{G}^{-1} \mathbf{U} \right) \mathbf{Q}^{MC} \\
&= \frac{c_2}{\sigma^2} \left(\mathbf{U} - \frac{c_2 M}{(\sigma^2 + c_2 M)} \mathbf{G} \mathbf{G}^{-1} \mathbf{U} \right) \mathbf{Q}^{MC} \\
&= \frac{c_2}{\sigma^2 + c_2 M} \mathbf{U} \mathbf{Q}^{MC}
\end{aligned} \tag{36}$$

$$\begin{aligned}
\mathbf{C}_\theta^{BQ}|_{c_1=0} &= c_2 \mathbf{G} - c_2^2 \mathbf{U} (0 * \mathbf{K}_s + c_2 \mathbf{K}_f + \sigma^2 \mathbf{I})^{-1} \mathbf{U}^\top \\
&= c_2 \mathbf{G} - c_2^2 \mathbf{U} (c_2 \mathbf{K}_f + \sigma^2 \mathbf{I})^{-1} \mathbf{U}^\top \\
&= c_2 \mathbf{G} - c_2^2 \mathbf{U} (c_2 \mathbf{U}^\top \mathbf{G}^{-1} \mathbf{U} + \sigma^2 \mathbf{I})^{-1} \mathbf{U}^\top \\
&= c_2 \mathbf{G} - c_2^2 \mathbf{U} \left(\frac{1}{\sigma^2} \mathbf{I} - \frac{c_2}{\sigma^4} \mathbf{U}^\top \left(\mathbf{G} + \frac{c_2}{\sigma^2} \mathbf{U} \mathbf{U}^\top \right)^{-1} \mathbf{U} \right) \mathbf{U}^\top \\
&= c_2 \mathbf{G} - \frac{c_2^2}{\sigma^2} \mathbf{U} \left(\mathbf{I} - \frac{c_2}{(\sigma^2 + c_2 M)} \mathbf{U}^\top \mathbf{G}^{-1} \mathbf{U} \right) \mathbf{U}^\top \\
&= c_2 \mathbf{G} - \frac{c_2^2}{\sigma^2} \left(\mathbf{U} - \frac{c_2 M}{(\sigma^2 + c_2 M)} \mathbf{G} \mathbf{G}^{-1} \mathbf{U} \right) \mathbf{U}^\top \\
&= \frac{\sigma^2 c_2}{\sigma^2 + c_2 M} \mathbf{G}
\end{aligned} \tag{37}$$

Thus, MC estimation is a special case of BQ when the state kernel k_s vanishes, i.e., the prior and posterior distributions over the state-value function $V_{\pi_{\theta}}$ (for $c_1 = 0$ in Eq. 30, 33) becomes non-existent. While encoding beneficial prior information in k_s is a non-trivial task, choosing a prior that is incapable of modeling the state-value function vastly limits the expressive power of the GP function approximation. This observation of ours is in agreement with previous works (Briol et al., 2015; Kanagawa et al., 2016, 2020; Bach, 2017) that prove a strictly faster convergence rate of BQ over MC methods, under mild regularity assumptions.

E.3 Relation between the Estimation Uncertainties of Vanilla PG and NPG

Empirically, we find that the optimal value of $c_2 \ll 1$, which has the following effect on the estimation uncertainty of Vanilla PG and Natural PG algorithms:

$$\mathbf{C}_{\theta}^{BQ} = c_2 \mathbf{G} - c_2^2 \mathbf{U} (c_1 \mathbf{K}_s + c_2 \mathbf{K}_f + \sigma^2 \mathbf{I})^{-1} \mathbf{U}^{\top} \approx c_2 \mathbf{G} \quad (38)$$

$$\mathbf{C}_{\theta}^{NBQ} = c_2 (\mathbf{G} + c_2 \mathbf{U} (c_1 \mathbf{K}_s + \sigma^2 \mathbf{I})^{-1} \mathbf{U}^{\top})^{-1} \approx c_2 \mathbf{G}^{-1}. \quad (39)$$

This observation is particularly interesting because for $c_2 \ll 1$, most uncertain gradient directions for vanilla PG approximately correspond to the most confident (least uncertain) directions for NPG. Crudely speaking, the natural gradient takes the step size along each direction and divides it by the estimated variance (from the gradient covariance matrix), which results in an inversion of the uncertainty. In contrast, UAPG divides the stepsize along each direction by the estimated standard deviation, which results in uniform uncertainty along all the directions. Moreover, for $c_2 \ll 1$, the ideal UAPG update for both vanilla PG and NPG converges along the $\mathbf{G}^{-\frac{1}{2}} \mathbf{L}_{\theta}^{BQ}$ direction.

F Importance of a Neural Network in the State kernel

We compare the performance of standard and deep RBF kernels for DBQPG (Fig. 5) and UAPG methods (Fig. 6) on two MuJoCo environments. We observe that the neural network (NN) feature extractor does not provide a significant advantage for DBQPG method that only uses the gradient mean \mathbf{L}_{θ}^{BQ} . On the other hand, deep kernels provide a consistent improvement for UAPG across all the continuous domains. From these observations, it can be inferred that one can obtain well-calibrated uncertainty estimates \mathbf{C}_{θ}^{BQ} by optimizing over an expressive family of covariance functions. Moreover, deep kernels have a negligible impact on the wall-clock time or memory usage and performs as good as, if not considerably better than, the corresponding base kernel.

G Implementation Details

Our policy π_{θ} comprises of a deep neural network that takes the environment’s state as input and estimates the mean and standard deviation of a normal distribution in the output action-space. We use the standard policy network architecture (Schulman et al., 2015; Duan et al., 2016) that comprises of a 2-layered fully-connected MLP with 64 hidden units and a tanh non-linearity in each layer. We use a neural network critic network that takes the environment’s state as input and models the state-value function $V_{\pi_{\theta}}$. We use the state-value predictions of the critic network for estimating the generalized advantage estimates \mathbf{A}^{GAE} (Schulman et al., 2016). The critic network consists of a 4-layered fully-connected MLP with 64, 48, 10, and 1 hidden units each layer. The first

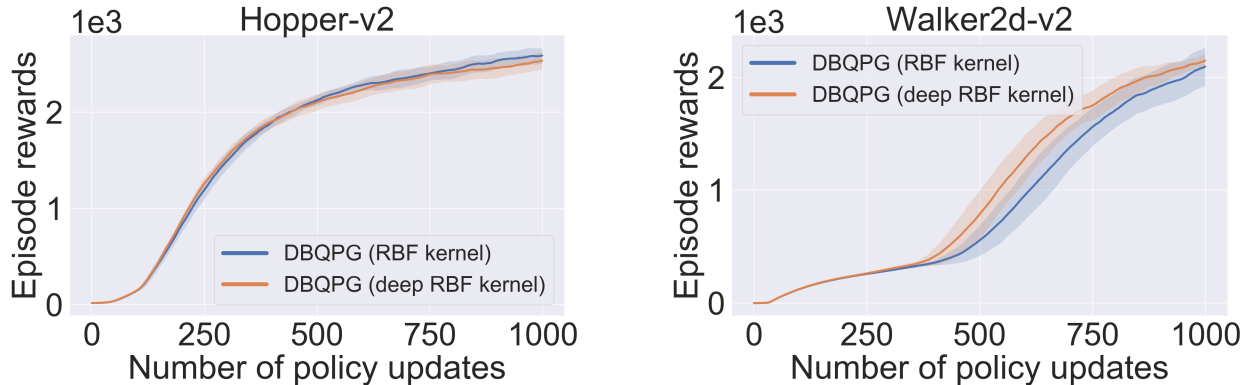


Figure 5: Standard vs deep RBF kernels using DBQPG method on Vanilla PG framework.

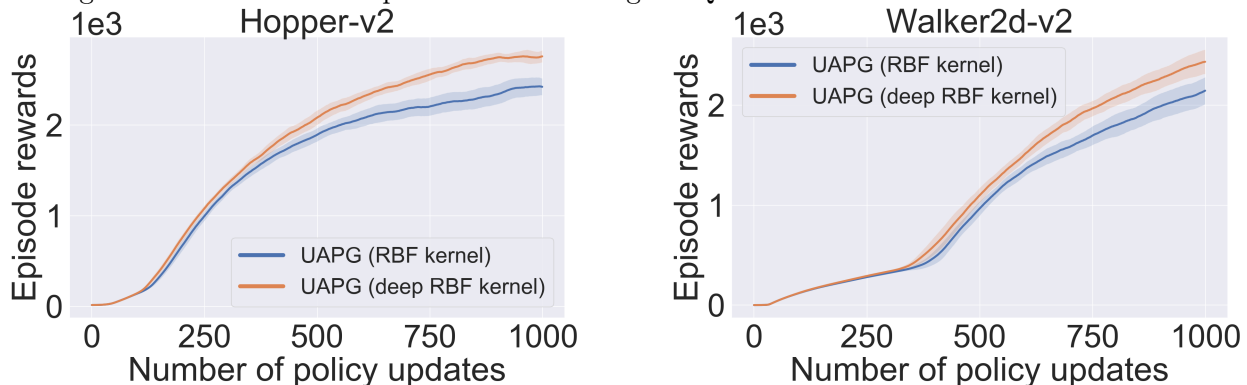


Figure 6: Standard vs deep RBF kernels using UAPG method on Vanilla PG framework.

three layers use a tanh non-linearity while the final layer which has no activation. Additionally we also have a GP function approximation that implicitly models the action-value function $Q_{\pi_{\theta}}$ with a fisher kernel (no additional hyperparameters) and a deep RBF state kernel (lengthscale + neural network parameters). Instead of using a new neural network feature extractor for the deep RBF kernel, we train a single linear layer on top of the pre-final layer (3^{rd} layer with 10 hidden units) of the critic network. The parameter sharing between the deep RBF kernel and critic network has a negligible effect on the agent’s performance, while needing significantly fewer parameters.

For structured kernel interpolation (Wilson & Nickisch, 2015), we use a grid size of 128 and impose an additive structure (i.e. the overall kernel is the sum of individual RBF kernels along each input dimension) on the deep RBF kernel. Additive structure allows us to take advantage of the Toeplitz method (Turner, 2010) for fast and scalable MVM computation. The GP’s noise variance σ^2 is set to 10^{-4} . In all the experiments of BQ-based methods, we fixed the hyperparameters $c_1 = 1$ and $c_2 = 5 \times 10^{-5}$ (tuned values). For optimizing the kernel parameters of the deep RBF kernel, we use *GPyTorch* (Gardner et al., 2018), a GPU-accelerated software platform for scalable GP inference. For UAPG method, increasing the SVD rank δ pushes the practical UAPG estimate closer to the ideal UAPG estimate, however, it also increases the GPU memory requirement. Thus, for each environment, we choose an estimate of δ that closely approximates the initial spectrum of estimation uncertainty \mathbf{C}_{θ}^{BQ} (Fig. 4) and also has a fa-

<i>Parameter</i>	<i>Value</i>	
Batch size	15000	
Discount factor γ	0.995	
GAE coefficient τ	0.97	
Trust region constraint / step size	0.01	
<i>Conjugate Gradient</i>	Max. CG iterations	50
	Residue (i.e., CG Threshold)	10^{-10}
	Damping (stability) factor	0.1

Table 1: Common hyperparameter setting across all the experiments.

vorable GPU memory consumption. Lastly, we set $\epsilon = 3$ for UAPG’s natural gradient update. Our implementation of DBQPG and UAPG methods is made publicly available at <https://github.com/Akella17/Deep-Bayesian-Quadrature-Policy-Optimization>.